Electronic Supplementary Material (ESI) for Chemical Communications.

< Supporting Information >

Harnessing Stress Granule Formation by Small-Molecules to Inhibit the Cellular Replication of SARS-CoV-2

Wan Gi Byun,[a] Jihye Lee,[b] Seungtaek Kim[b] and Seung Bum Park*[,a]

* Corresponding authors

[a] CRI Center for Chemical Proteomics, Department of Chemistry, Seoul National University, Seoul 08826, Korea

[b] Zoonotic Virus Laboratory, Institut Pasteur Korea, Seongnam 13488, Korea

*E-mail: sbpark@snu.ac.kr

1. Extended Materials and Methods

Chemistry

The ^{1}H and ^{13}C NMR spectra were recorded on a AVANCE 600 [Bruker] or Varian Inova-500 [Varian Associates], and chemical shifts were measured in ppm referenced to tetramethylsilane (TMS, 0 ppm) as an internal standard. Multiplicity was indicated as follows: s (singlet); d (doublet); t (triplet); q (quartet); m (multiplet); dd (doublet of doublet); dt (doublet of triplet); td (triplet of doublet); qd (quartet of doublet); quind (quintet of doublet); tdd (triplet of doublet of doublet); brs (broad singlet), etc. Coupling constants were reported in Hz. Low-resolution mass spectrometry (LRMS) was conducted by LCMS-2020 [Shimadzu]. High-resolution mass spectrometry (HRMS) analysis were performed with Orbitrap Exploris 120 [ThermoFisher Scientific] at the Department of Chemistry, Seoul National University. All solvents and organic reagents were purchased from commercial venders and used without further purification unless otherwise mentioned. Synthetic methods for compounds used in this study were previously reported.[1]

Purity determination from HPLC analysis

Reverse-phase high performance liquid chromatography (HPLC) analysis was conducted on an analytical LC-MS, LCMS-2020 [Shimadzu], equipped with a YMC-Triart C18 column (TA12S05-1546WT, 150×4.6 mm ID, S-5 μm, 12 nm). HPLC solvents consist of water containing 0.1% formic acid (solvent A) and acetonitrile containing 0.1% formic acid (solvent B). HPLC spectra were obtained on the basis of the absorbance at 254 nm, and the purities of final synthesized compounds were confirmed on the basis of the HPLC peak area. Samples were analyzed starting from 10% B in A to 100% B for 25 min.

Cell culture and transfection

G3BP1-GFP expressed U2OS human osteosarcoma epithelial cell was kindly provided by Prof. Jin-A Lee, Hannam University. Calu-3 human airway epithelial cells and Vero kidney epithelial cells from African green monkey were obtained from the Korean Cell Line Bank [KCLB] (KCLB No.30055 and No.10081, respectively). G3BP1-GFP expressed U2OS, Calu-3, and Vero cells were maintained in DMEM medium [Welgene] supplemented with 10% heat-inactivated fetal bovine serum (FBS) [Gibco], 1% antibiotic-antimycotic solution [Gibco] in a humidified 5% CO_2 atmosphere at 37 °C. After complete adhesion, cells were transfected using pre-complexed poly(I:C) (HMW)/LyoVec^{TM} reagent [InvivoGen]. For authentic SARS-CoV-2 experiments, Calu-3 used in this study is a clonal isolate, which shows higher growth rate compared with the parental Calu-3 obtained from the American Type Culture Collection [ATCC] [ATCC HTB-55]. Calu-3 was maintained at 37 °C with 5% CO_2 in EMEM [ATCC] supplemented with 20% heat-

inactivated FBS, 1% MEM-non-essential amino acid solution [Gibco] and 2% antibiotic-antimycotic solution [Gibco]. Vero cell was obtained from the American Type Culture Collection [ATCC] (ATCC CCL-81 and C1008, respectively) and maintained at 37 °C with 5% CO_2 in DMEM [Welgene], supplemented with 10% heat-inactivated FBS and 2% antibiotic-antimycotic solution [Gibco].

Western blot

Calu-3 cells were seeded into 12-well plates at a density of 3.5×10^5 cells/well. After complete adhesion, cells were treated as described in the texts and figures. The cells were washed with PBS, lysed using RIPA buffer (50 mM Tris–HCl, pH 7.8, 150 mM NaCl, 1% NP-40, 0.5% deoxycholate, 5 mM NaF, 2 mM Na_3VO_4, 1× protease inhibitor cocktail [Roche]), and the concentration of total protein was measured by Pierce BCA protein assay kit [ThermoFisher Scientific]. Proteins were resolved by SDS-PAGE, transferred to PVDF membrane [Bio-Rad], and blocked with 2% bovine serum albumin (BSA) [MP Biomedicals] in Tris buffered saline with Tween20 (TBST) [Sigma]. Membranes were probed with protein-specific antibodies (PKR, Santa Cruz #sc-6282; phospho-PKR, Abcam #ab32036; eIF2α, Santa Cruz #sc-133132; phopho-eIF2α, Abcam #ab32157; IRF3, Cell Signaling Technology #4302S; phospho-IRF3, Abcam #ab76493; puromycin, Merck Millipore #MABE343; GAPDH, Cell Signaling Technology #2118S).

Stress granule imaging by immunofluorescence

Calu-3 cells were seeded into 96-well black-sided, clear bottom plates at a density of 4×10^4 cells/well. Vero cells were seeded into 96-well black-sided, clear bottom plates at a density of 1×10^4 cells/well. After complete adhesion, cells were treated as described in the main text and figures. Poly(I:C) was treated for 5 h before compound treatments. After washed with PBS, the cells were fixed with 4% paraformaldehyde (PFA) in PBS for 20 min at room temperature and permeabilized with 0.5% Triton X-100 at 4 °C for 20 min. Cells were then washed with PBS three times, blocked with 3% BSA in PBS for 1 h and treated with anti-G3BP1 primary antibodies at 4 °C overnight (Santa Cruz, #sc-81940). After washed with PBS, cells were applied with Alexa 488-conjugated anti-mouse secondary antibody (Abcam, #ab150113), and nucleus was stained with Hoechst 33342 in PBS (1:5000) for 30 min. Cells were photographed using IN Cell Analyzer 2000 or IN Cell Analyzer 2500 [GE Healthcare]. Images were analyzed to quantify stress granule puncta per cell using Developer software [GE Healthcare]. On average, 6,042 cells for Calu-3 cell line and 1,761 cells for Vero cell line were analyzed for each technical replicate. All data are presented as mean ± standard deviation (SD) from two independent biological replicates each consisting of at least two technical replicates.

Stress granule monitoring and compound screening using G3BP1-GFP expressed U2OS cell line

G3BP1-GFP expressed U2OS cells were seeded into 96-well black-sided, clear bottom plates at a density of 1.0×10^4 cells/well for 24 h. Cells were transfected with 1.25 μg/mL poly(I:C) (HMW)/LyoVec^{TM} in the order of well-imaging. After 5-h incubation, nuclei were stained by medium-diluted Hoechst 33342 [ThermoFisher] for 30 min. Plates were scanned in an IN Cell Analyzer 2000 [GE Healthcare] at $\lambda_{ex}/\lambda_{em}$ = 490/525 nm (for FITC channel) for Venus fluorescence and at $\lambda_{ex}/\lambda_{em}$ = 350/455 nm (for DAPI channel) for nuclei. Then, 464-membered pDOS library compounds were treated using multichannel pipette (at 10 μM concentration, 0.5% DMSO) in the order of image acquisition. Plates were scanned after 40, 100, 160, 220, and 280 min on the addition of compounds. Bright-field images were also taken to check the cell morphologies and compound aggregates. Images were analyzed to quantify total count of stress granules per cell using Developer software [GE Healthcare]. On average, 610 cells were analyzed from two different fields for each compound. Each value of total stress granules over cell was normalized to that of 0 min and DMSO controls. Graph for the change of the number of stress granules on the time and compound was plotted using OriginPro 8.5 [OriginLab].

Cell Viability Assay

Cells were seeded in 96-well plates at a density of 4×10^4 cells/well and grown overnight. After complete adhesion, cells were treated with various concentrations of **C01**–**C04**. After 24 h, the media were exchanged to water-soluble tetrazolium (WST) [DoGen]-containing media, and plates were incubated for 2 h in a humidified 5% CO_2 atmosphere at 37 °C. The absorbance at 455 nm was recorded by BioTek Synergy HTX Microplate reader. The percentage of viability was calculated by using the following equation: Viability (%) = (absorbance in treated wells)/(absorbance in control wells) × 100. Background absorbance value was subtracted.

RNA extraction and quantitative real-time PCR

Calu-3 cells were seeded into 12-well plates at a density of 3.5×10^5 cells/well. After complete adhesion, cells were treated as described in the main text and figures. Poly(I:C) was treated for 5 h before compound treatments. Total RNA was extracted using the RNeasy kit [Qiagen] according to the manufacturer's protocols. cDNAs were prepared with AccuPower CycleScript RT PreMix dT20 [Bioneer] according to the manufacturer's protocols. qRT-PCR experiments were performed using KAPA SYBR FAST ABI Prism qPCR Master Mix [KAPA Biosystems]. The data were analyzed by the comparative Ct method and normalized against housekeeping

gene, GAPDH. All data are presented as mean ± standard deviation from at least two independent biological replicates.

Virus

SARS-CoV-2 (βCoV/KOR/KCDC03/2020) was provided by Korea Disease Control and Prevention Agency (KDCA), and was propagated in Vero E6 cells. Viral titers were determined by plaque assays in Vero cells. All experiments using SARS-CoV-2 were performed at Institut Pasteur Korea in compliance with the guidelines of the Korea National Institute of Health (KNIH), using enhanced biosafety level 3 (BSL-3) containment procedures in laboratories approved for use by the Korea Disease Control and Prevention Agency (KDCA).

Antiviral test and dose-response curve (DRC) analysis by immunofluorescence

Vero cells were seeded at 1.2×10^4 cells per well with DMEM [Welgene] supplemented with 2% heat-inactivated FBS and 2% antibiotic-antimycotic solution [Gibco] in a black, 384-well, μClear plates [Greiner Bio-One] for 24 h before the experiment. Calu-3 cells were seeded at 2.0×10^4 cells per well with EMEM [ATCC] supplemented with 20% heat-inactivated FBS, 1% MEM-non-essential amino acid solution [Gibco] and 2% antibiotic-antimycotic solution [Gibco] in a black, 384-well, μClear plates [Greiner Bio-One] for 24 h before the experiment. Ten-point DRCs were generated with two-fold dilutions, with compound concentrations ranging from 0.1 to 50 μM. For viral infection, plates were transferred into the BSL-3 containment facility and SARS-CoV-2 was added at a multiplicity of infection (MOI) of 0.0125 for Vero cells and 0.2 for Calu-3 cells. The plates were incubated at 37 ºC for 24 h. The cells were fixed at 24 h post infection (hpi) with 4% PFA, permeabilized with 0.25% Triton X-100 solution. Anti-SARS-CoV-2 nucleocapsid (N) primary antibody (Sino Biological, #40143-T62), Alexa 488-conjugated goat anti-rabbit IgG secondary antibody (Molecular Probes, #MOP-A-11034), and Hoechst 33342 [Molecular Probes] were treated to the tested cells for immunofluorescence. The images acquired with Operetta high-throughput imaging device [Perkin Elmer] were analyzed using the Columbus software [Perkin Elmer] to quantify cell numbers and infection ratios. The infection ratio of each well was normalized using the average infection ratio of infection control (0.5% DMSO) and the average infection ratio of non-infection control (Mock), which were set 0% and 100% inhibition of infection, respectively. Dose-response curves (DRCs) were generated using Prism7 software [GraphPad]. Half-maximal inhibitory concentration (IC_{50}) values were calculated using the following equation: $Y = Bottom + (Top - Bottom)/(1 + (IC_{50}/X)^{Hillslope})$, using XLfit 4 Software. All IC_{50} and 50% cytotoxic concentration (CC_{50}) values were measured in duplicate, and the quality of each assay was controlled by Z′-factor and the coefficient of variation in percent (%CV).

Co-immunofluorescence

Vero cells were seeded at a density of 3.5×10^4 cells per well in a 96-well plates, µClear plates [Greiner Bio-One] at 24 h prior to the experiment. Compounds were added to cells in each well. Subsequently, the cells were infected with SARS-CoV-2 at 5 MOI. At 5 hpi, the cells were fixed with 4% PFA, permeabilized with 0.25% Triton X-100 solution and stained using mouse monoclonal antibody to G3BP1 (Santa Cruz, #sc-81940) and rabbit polyclonal antibody to SARS-CoV-2 N (Sino Biological, #40143-T62). Then, Alexa 488-conjugated goat anti-rabbit IgG secondary antibody (Molecular Probes, #MOP-A-11034), Alexa Fluor Plus 647-conjugated goat anti-mouse IgG secondary antibody (Invitrogen, #A32728) and Hoechst 33342 [Molecular Probes] were treated to the cells. Cells were imaged with Operetta high-throughput imaging device [Perkin Elmer].

Drug combination assay

Vero cells were seeded at 1.2×10^4 cells per well with DMEM [Welgene] supplemented with 2% heat-inactivated FBS and 2% antibiotic-antimycotic solution [Gibco] in a black, 384-well, µClear plates [Greiner Bio-One] 24 h before the experiment. Ten-point DRCs were generated with a 2/3-fold serial dilution, with compound concentrations ranging from 0.78 to 30 µM. Final 10 and 15 µM of lopinavir or DMSO were added. For viral infection, plates were transferred into the BSL-3 containment facility and SARS-CoV-2 was added at 0.0125 MOI. The plates were incubated at 37 ºC for 24 h. The cells were fixed at 24 hpi with 4% PFA, permeabilized with 0.25% Triton X-100 solution. Anti-SARS-CoV-2 N primary antibody (Sino Biological, #40143-T62), Alexa 488-conjugated goat anti-rabbit IgG secondary antibody (Molecular Probes, #MOP-A-11034), and Hoechst 33342 were treated to the cells for immunofluorescence. The images acquired with Operetta high-throughput imaging device [Perkin Elmer] were analyzed using the Columbus software [Perkin Elmer] to quantify cell numbers and infection ratios. The infection ratio of each well was normalized using the average infection ratio of infection control (1% DMSO) and the average infection ratio of non-infection control (Mock), which were set 0% and 100% inhibition of infection, respectively. DRCs were generated using Prism7 software (GraphPad). IC_{50} values were calculated using the following equation: $Y = Bottom + (Top - Bottom)/(1 + (IC_{50}/X)^{Hillslope})$, using XLfit 4 Software. All IC_{50} and CC_{50} values were measured in duplicate.

2. Supplementary data

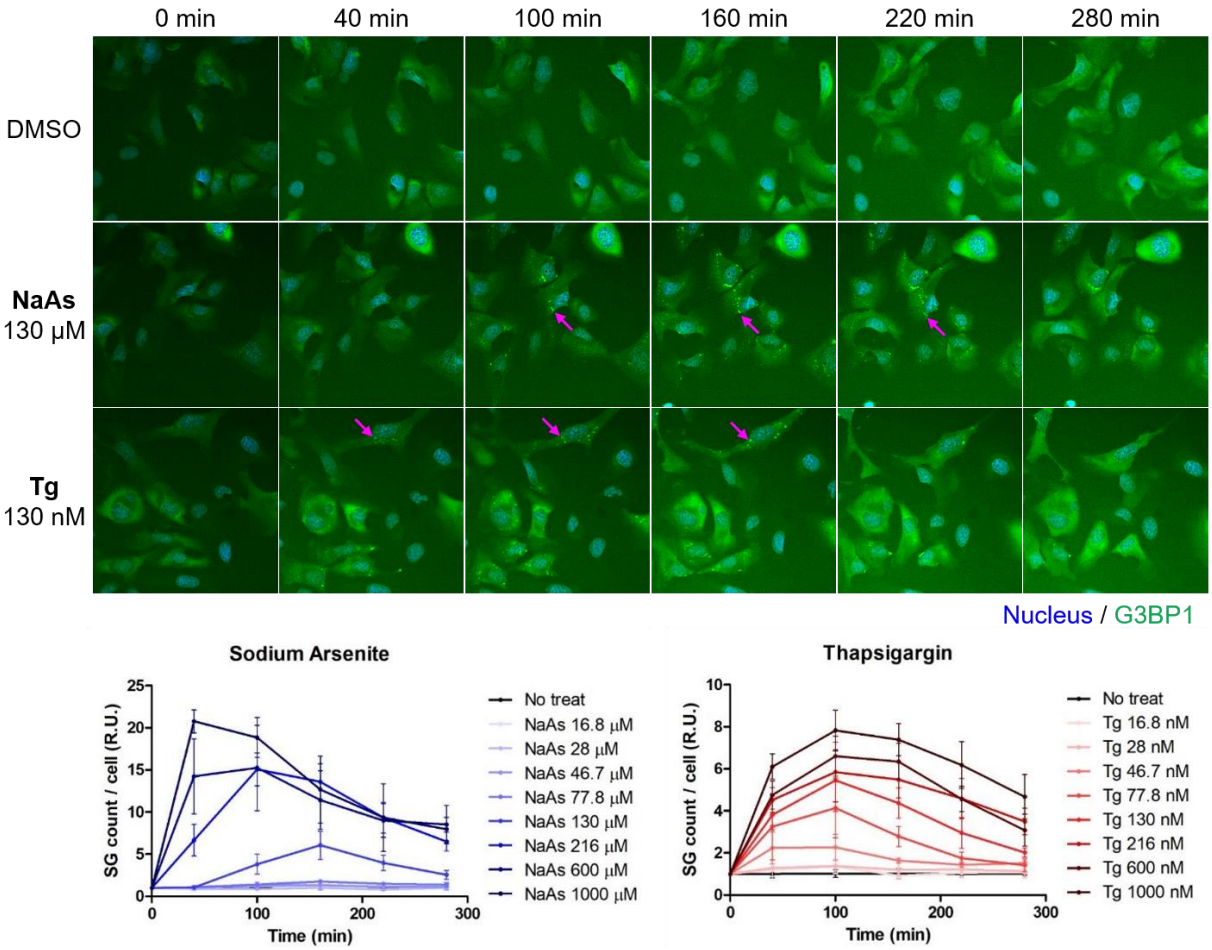

Figure S1. Time-course stress granule monitoring upon treatment of known stress granule enhancers, sodium arsenite (NaAs) and thapsigargin (Tg), using G3BP1-GFP-expressed U2OS cells. Magenta arrows indicate examples of stress granules. Data represent mean ± SD from three replicates.

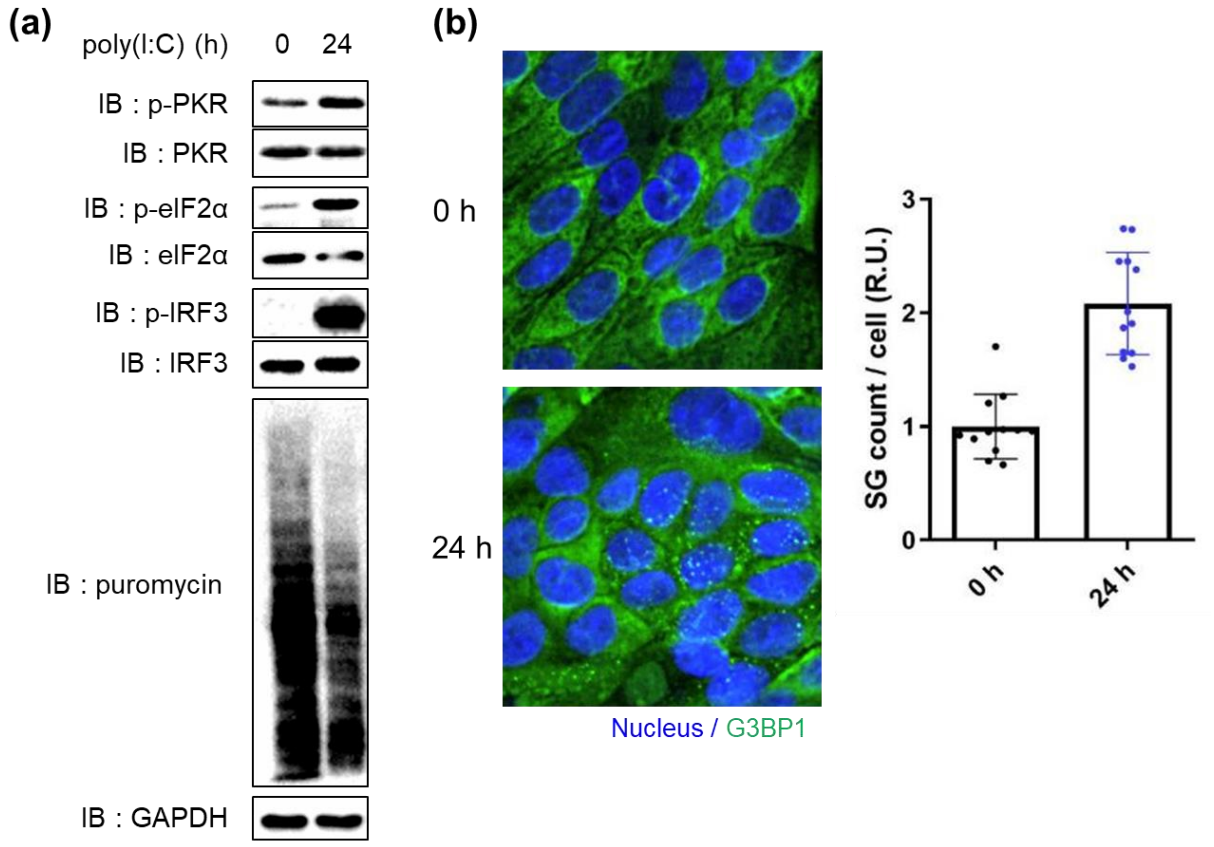

Figure S2. (a) Activation of innate antiviral response in Calu-3 cell. (b) Stress granule formation induced by poly(I:C) in Calu-3 cell. 10 μg/mL of poly(I:C) was treated. Data represent mean ± SD. n=12 from two independent biological replicates.

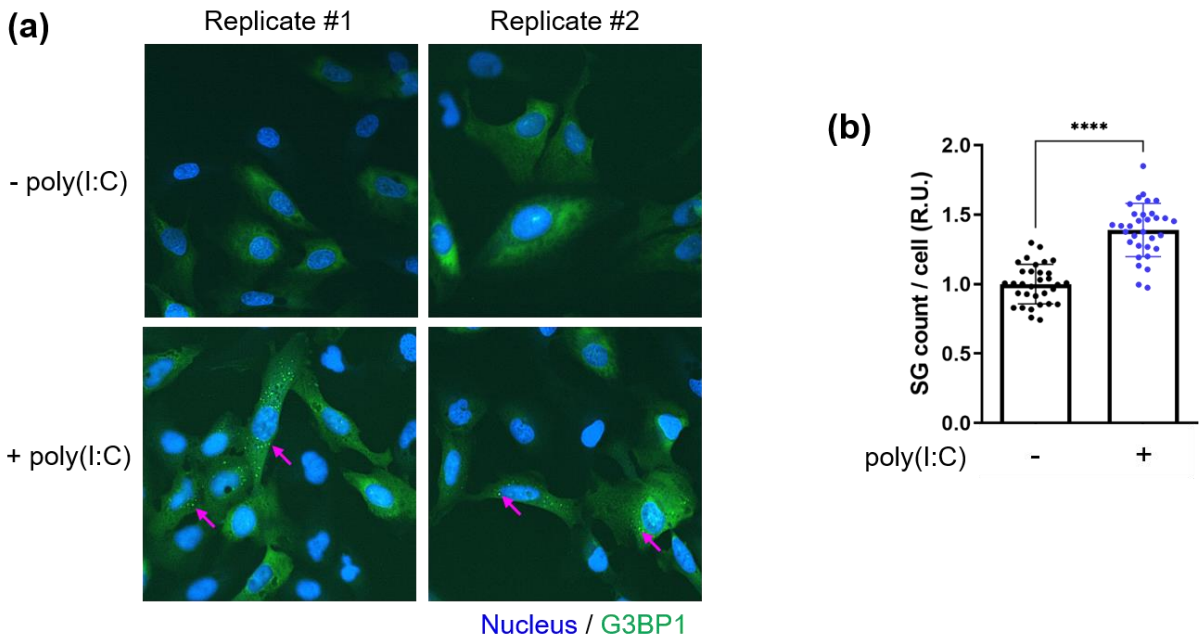

Figure S3. Stress granule formation induced by poly(I:C) in G3BP1-GFP-expressed U2OS cells. (a) Representative images. 1.25 μg/mL of poly(I:C) was transfected to cells for 5 h, the same condition as the compound screening. Magenta arrows indicate examples of stress granules. (b) Quantification data of resulting images. Data represent mean ± SD of 32 replicates. ****p < 0.0001 (Student's *t* test).

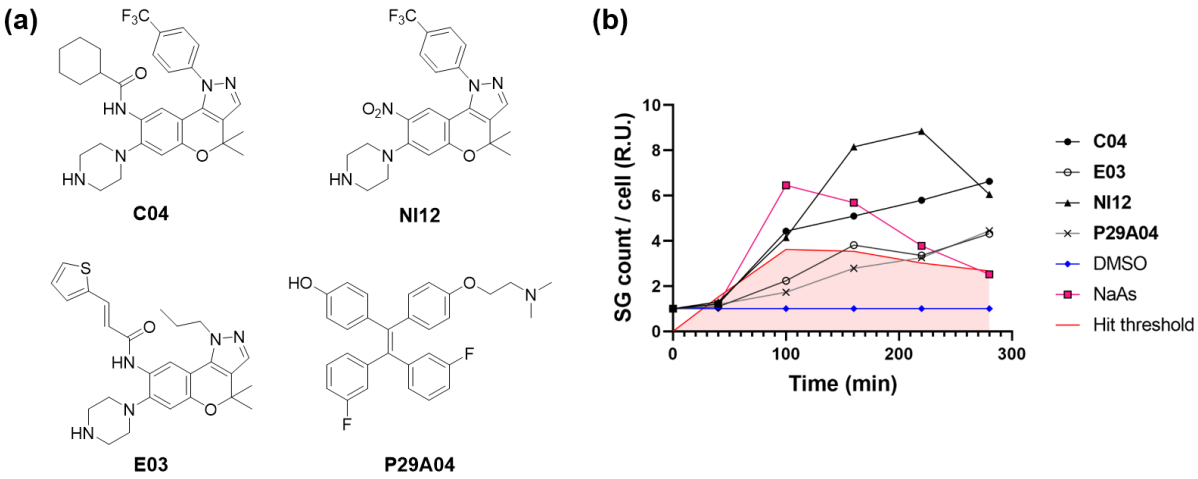

Figure S4. (a) Chemical structures of hit compounds and (b) their time-course stress granule screening results. Data represent the mean value of images obtained from two different fields.

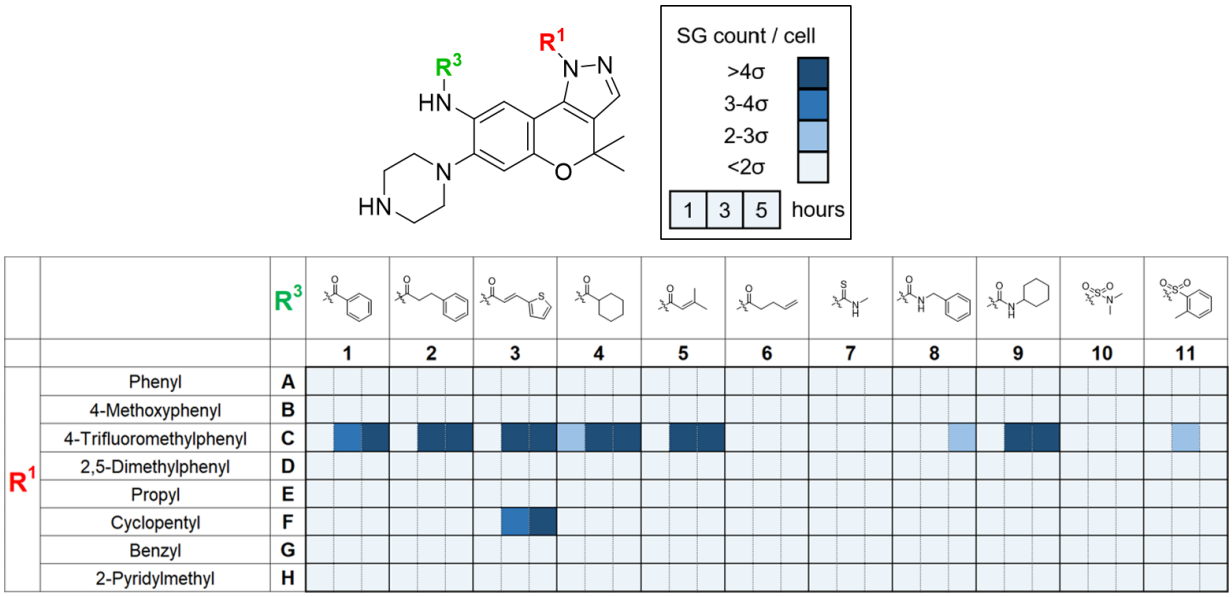

Figure S5. Structure-activity relationship study. After transfection of G3BP1-GFP-expressed U2OS cells with 1.25 μg/mL poly(I:C), 5 μM compounds were treated.

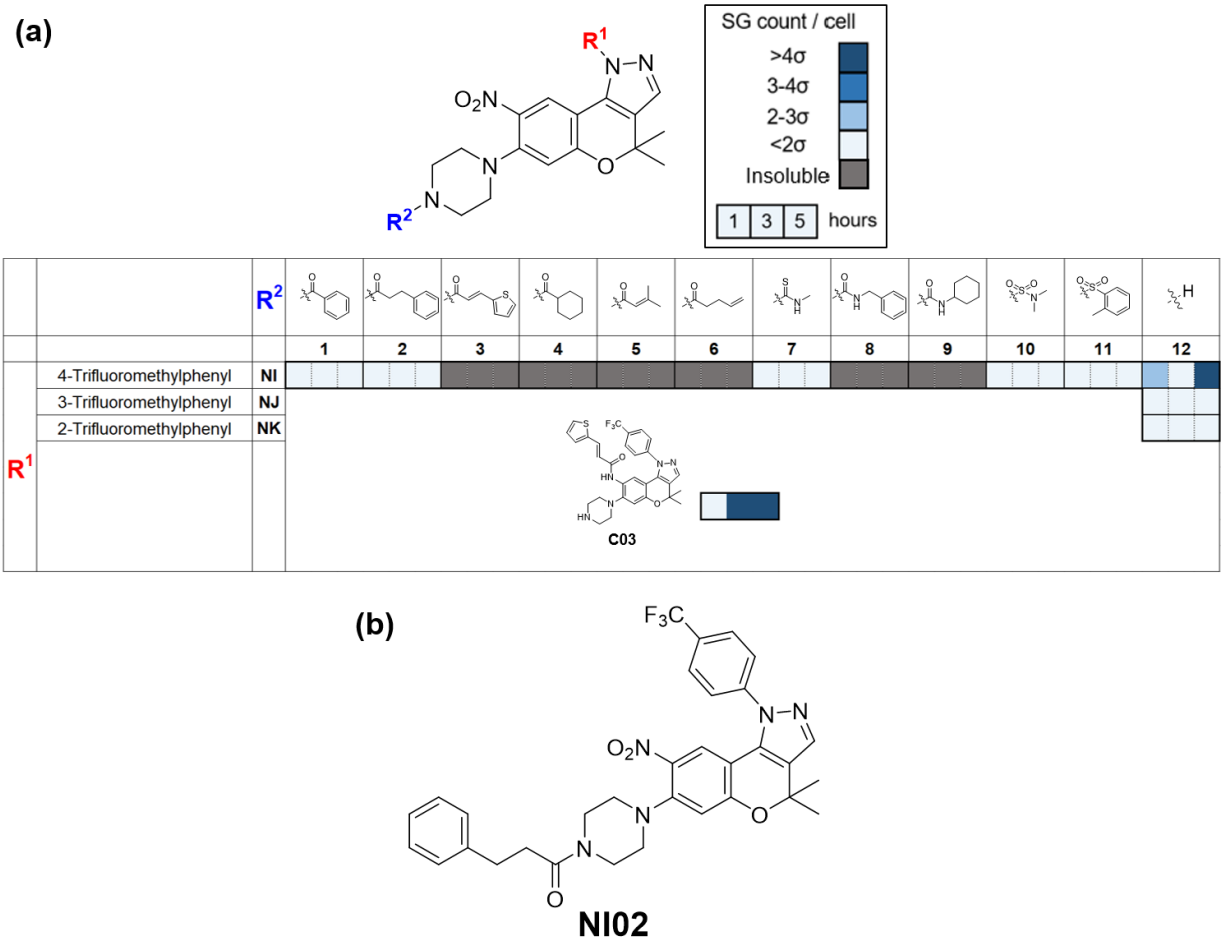

Figure S6. (a) Structure-activity relationship study at the R^3 position and the substituted position (*ortho*-, *meta*-, and *para*-) of trifluoromethyl group. After transfection of 1.25 μg/mL poly(I:C), 5 μM compounds were treated. (b) Chemical structure of a selected negative compound, **NI02**, for further biological evaluations.

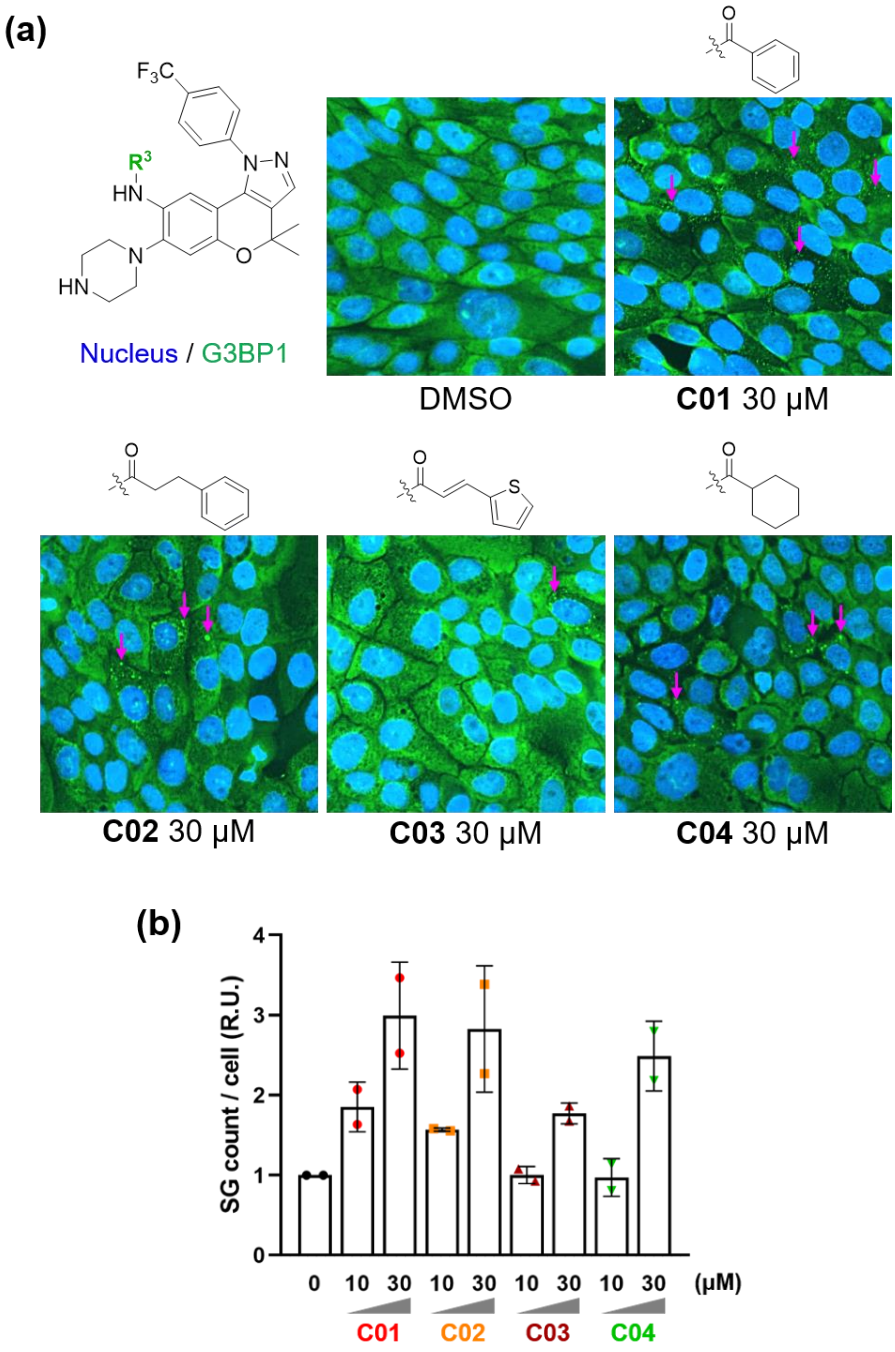

Figure S7. Dose-dependent induction of stress granules in Calu-3 cells. (a) Representative immunofluorescence images of G3BP1 in 5 h after transfection of 2.5 µg/mL poly(I:C). Magenta arrows indicate examples of stress granules. (b) Quantification data of resulting images. Data represent mean ± SD from two independent biological replicates.

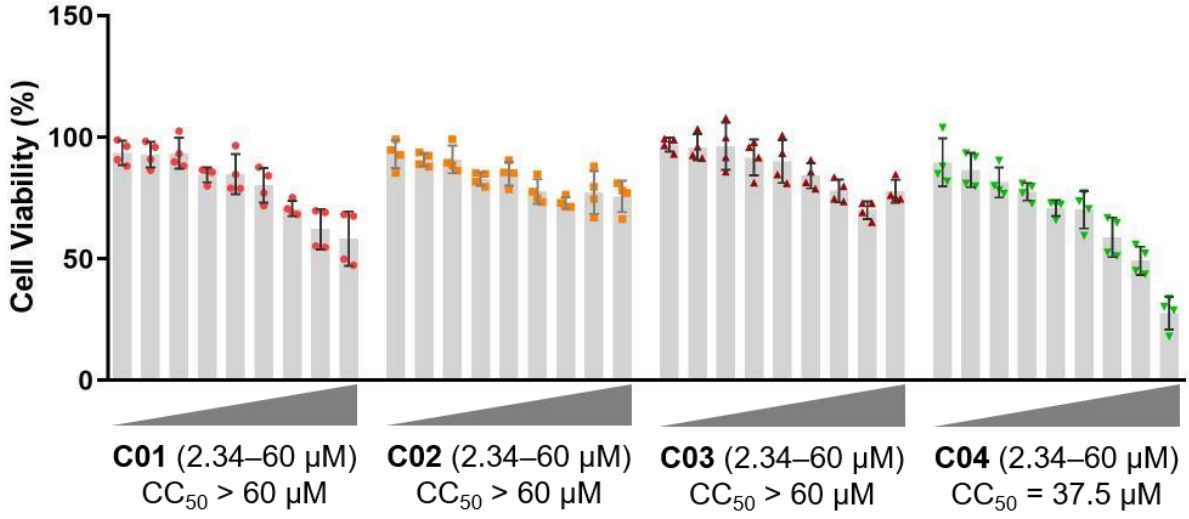

Figure S8. Cell viability assay for **C01**–**C04** in Calu-3 cells. After complete adhesion, cells were treated with various concentrations of compounds for 24 h. Data represent mean ± SD. n=4 from two independent biological replicates.

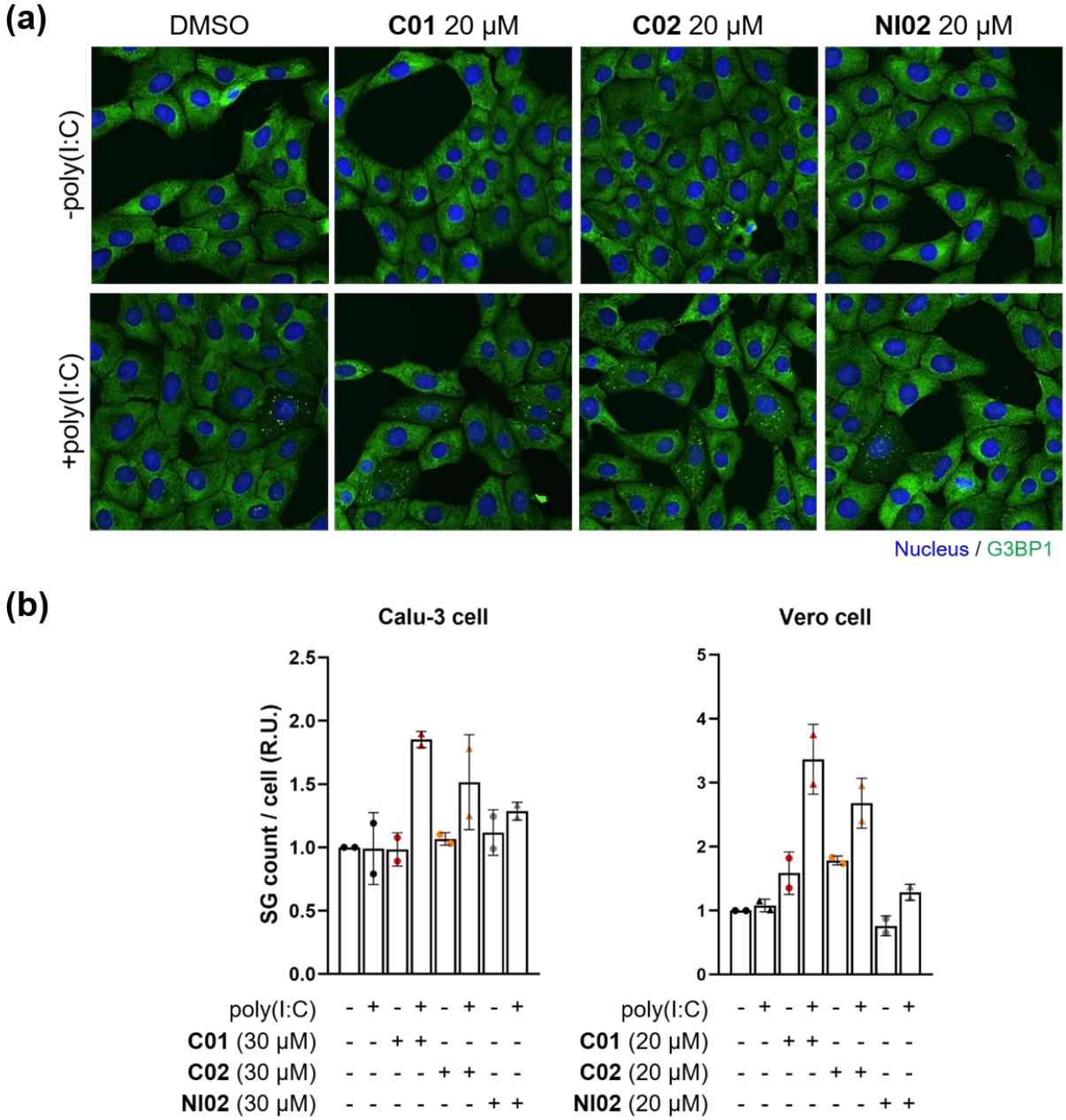

Figure S9. poly(I:C)-dependent induction of stress granule formation. (a) Representative images of immunofluorescence against G3BP1 in Vero cells. (b) Quantification data of immunofluorescence assay in Calu-3 and Vero cells. 2.5 μg/mL of poly(I:C) was used. Data represent mean ± SD from two independent biological replicates.

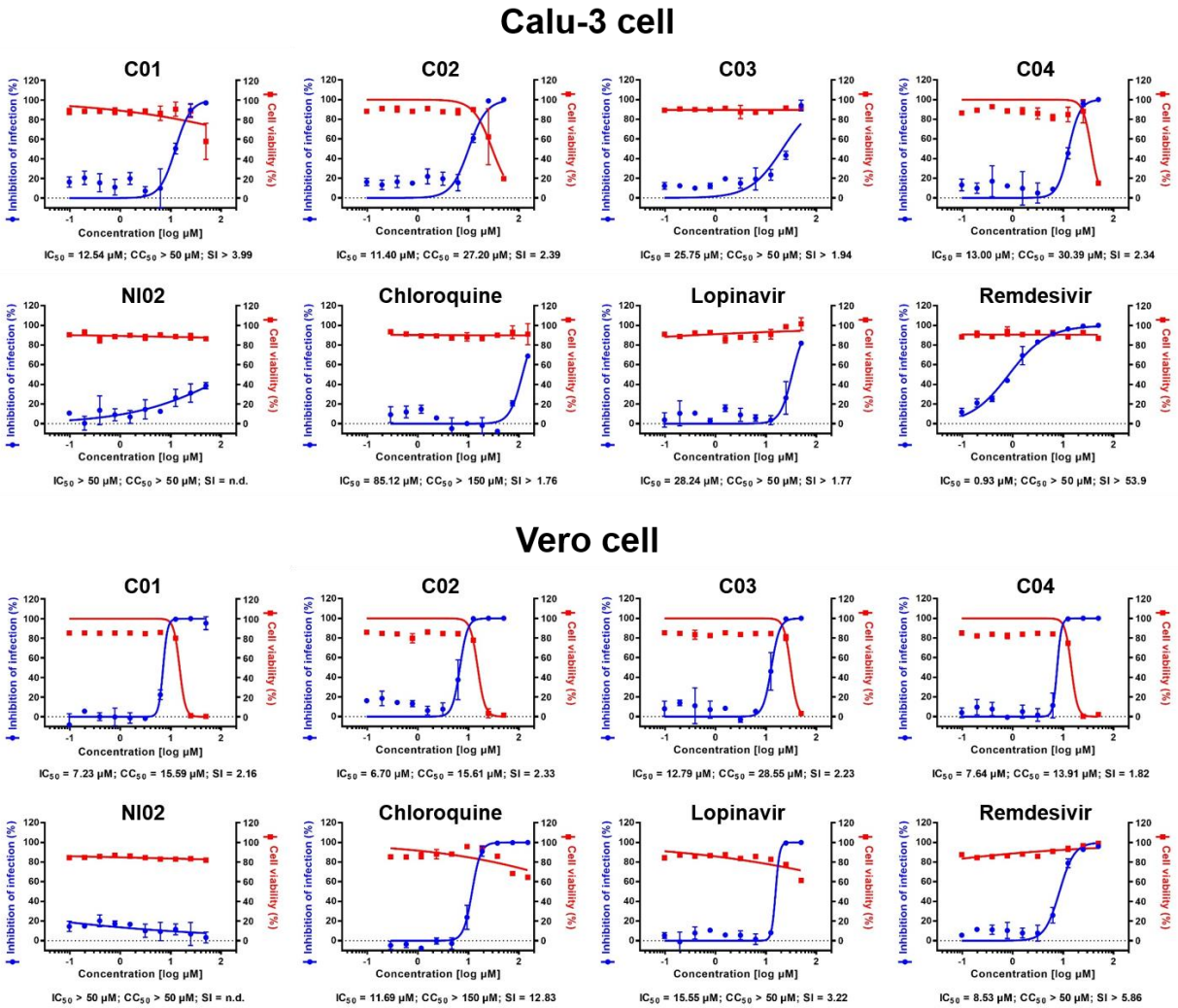

Figure S10. Dose-response curves (DRCs) of tested compounds in Calu-3 and Vero cells. Ten-point DRCs were generated. Calu-3 and Vero cells were infected with SARS-CoV-2 at a multiplicity of infection (MOI) of 0.2 and 0.0125, respectively. Then, various concentrations of compounds were added. After 24 h post infection, immunofluorescence detections of SARS-CoV-2 N protein and host nucleus were performed to quantitatively measure the inhibition of viral infection as well as cell viability. The blue line indicates the inhibition of SARS-CoV-2 infection, and the red line indicates cell viability. Data represent mean ± SD from two independent biological replicates.

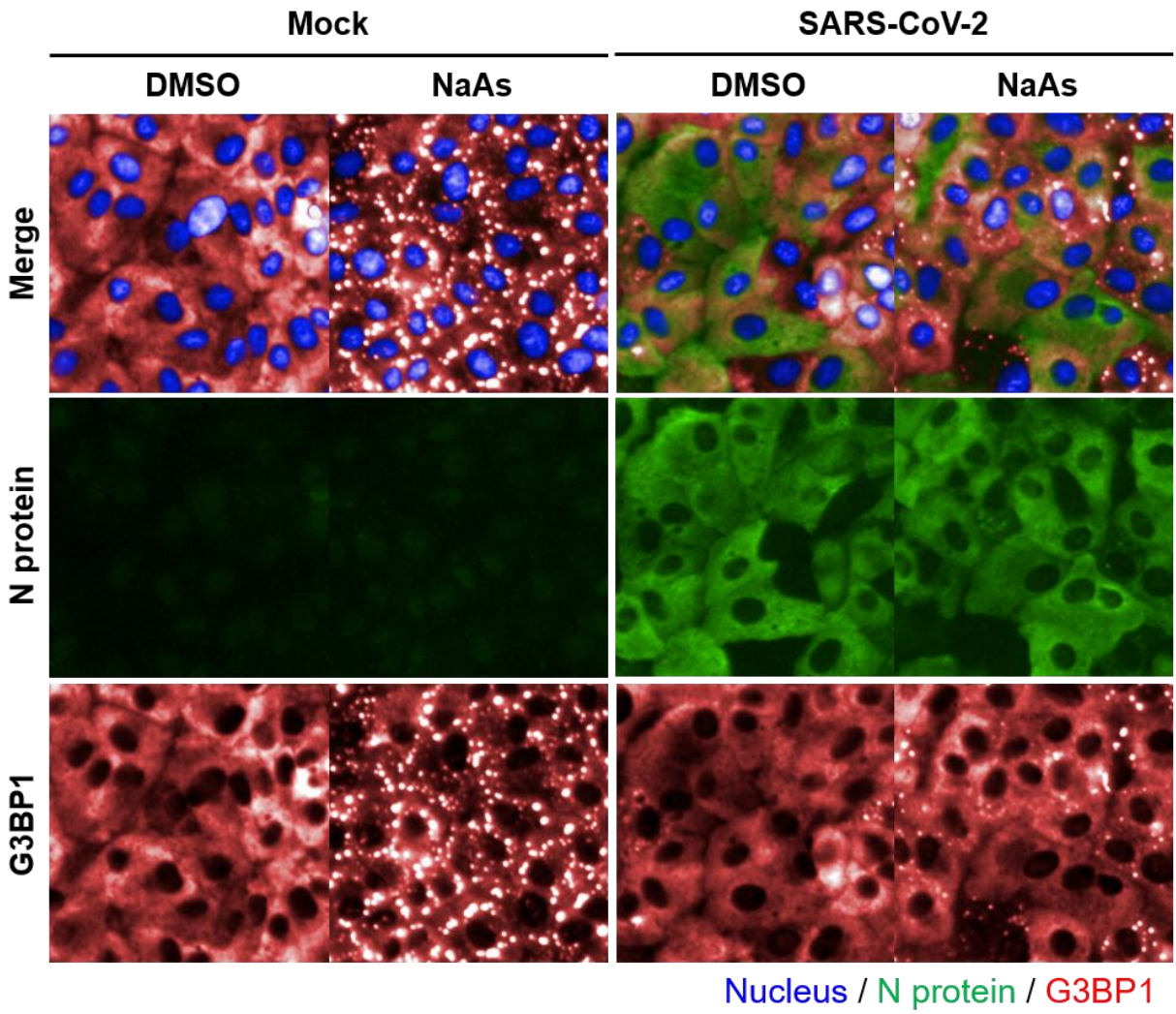

Figure S11. Co-immunofluorescence assay in Vero cells. Cells were infected with SARS-CoV-2 at 5 MOI or mock, and treated with 250 μM of sodium arsenite (NaAs) for 1 h before fixation. Then, immunofluorescence detections of nucleus, SARS-CoV-2 N protein, and G3BP1 were performed. Puncta in G3BP1 images were shown in white color due to the signal saturation. We can clearly observe the enhancement of stress granule formation in the presence of NaAs. But NaAs-induced stress granule formation was significantly reduced by the SARS-CoV-2 infection.

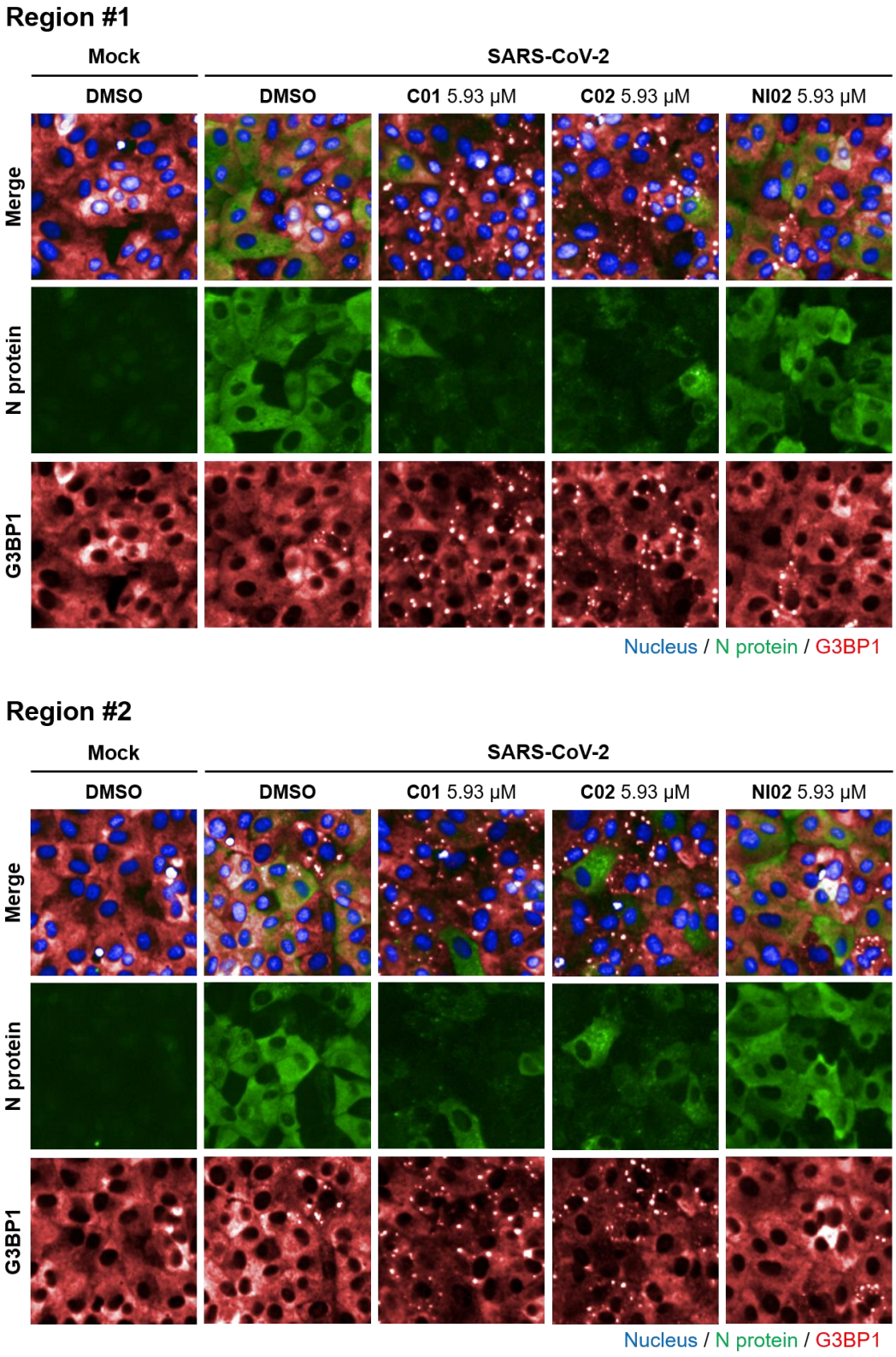

Figure S12. Co-immunofluorescence assay in Vero cells. Cells were infected with SARS-CoV-2 at 5 MOI or mock, and treated with 5.93 μM of compounds for 5 h before fixation. Then, immunofluorescence detections of nucleus, SARS-CoV-2 N protein and G3BP1 were performed.

(a)

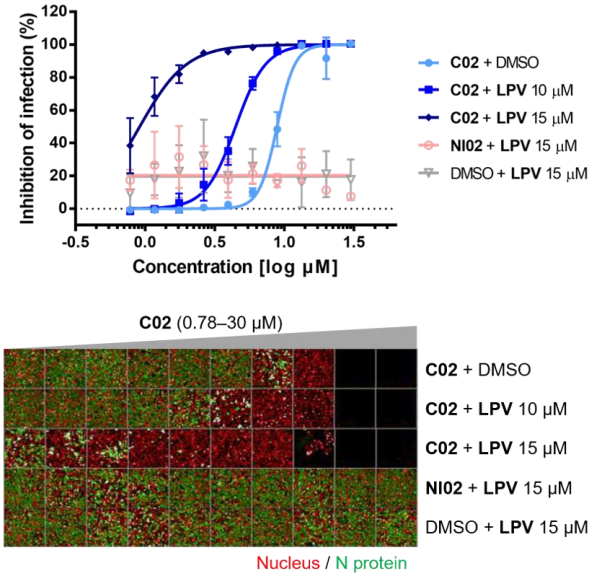

(b)

Compound	IC_{50} (µM)	CC_{50} (µM)	Selective Index*
C01 + DMSO	7.64	15.97	2.09
C01 + **LPV** 10 µM	3.21	14.58	4.54
C01 + **LPV** 15 µM	<0.78	13.97	>17.91
C02 + DMSO	8.85	14.68	1.66
C02 + **LPV** 10 µM	4.45	14.25	3.20
C02 + **LPV** 15 µM	0.89	12.28	13.80
NI02 + DMSO	>30	>30	n.d.**
NI02 + **LPV** 10 µM	>30	>30	n.d.
NI02 + **LPV** 15 µM	>30	>30	n.d.
LPV	17.27	>50	>2.90
Chloroquine	11.35	>150	>13.22
Remdesivir	8.21	>50	>6.09

*Selective Index = CC_{50}/IC_{50}; **n.d., not determined.

Figure S13. Drug combination assay in Vero cells. (a) Co-treatment of **C02** with lopinavir (**LPV**). (b) Values obtained from drug combination assay. Ten-point DRCs were generated. Briefly, Vero cells were infected with SARS-CoV-2 at a multiplicity of infection (MOI) of 0.0125, then various concentrations of compounds in the absence or presence of lopinavir (10 or 15 µM) were added. At 24 h post infection, immunofluorescence detections of SARS-CoV-2 N proteins and host nucleus were performed to quantitatively measure the inhibition of viral infection as well as cell viability.

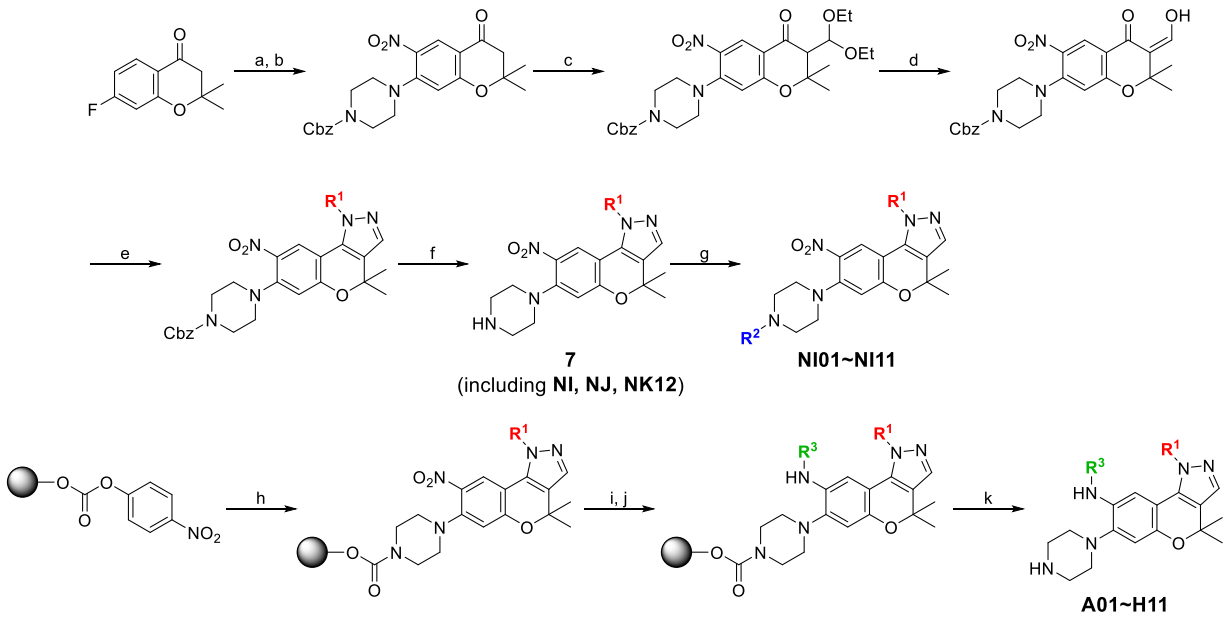

Scheme S1. Synthesis of diverse benzopyranylpyrazoles.[1] (a) KNO_3, H_2SO_4, 0 °C, 2 h; (b) Cbz-piperazine, acetonitrile, 40 °C, overnight; (c) $HC(OEt)_3$, $BF_3{\cdot}OEt_2$, DIPEA, dichloromethane, -78 °C to r.t., 2 h; (d) I_2, acetone, 35 °C, overnight; (e) substituted hydrazines, AcOH, 35 °C; (f) 40% KOH, tetrahydrofuran, EtOH or Me_2S, $BF_3{\cdot}OEt_2$, dichloromethane; (g) chemical modification with i) carboxylic acids, DIC, DIPEA, DMAP, dichloroethane or ii) isocyanates, dichloroethane or iii) isothiocyanates, dichloroethane or iv) sulfonyl chlorides, pyridine/dichloroethane = 1/2; (h) benzopyranylpyrazoles **7**, dimethylformamide, 24 h; (i) 2 M $SnCl_2{\cdot}(H_2O)_2$ in dimethylformamide; (j) carboxylic acids, PyBOP, DMAP, 3% NMM in dimethylformamide, 24 h or isocyanates, TEA, dichloroethane, 24 h or sulfonyl chlorides, pyridine/DCE = 1/2, 24 h; (k) 50% TFA in dichloromethane, 1 h.

	Calu-3			Vero		
Compound	IC_{50} (μM)	CC_{50} (μM)	Selective Index*	IC_{50} (μM)	CC_{50} (μM)	Selective Index
C01	12.54	>50	>3.99	7.23	15.59	2.16
C02	11.40	27.20	2.39	6.70	15.61	2.33
C03	25.75	>50	>1.94	12.79	28.55	2.23
C04	13.00	30.39	2.34	7.64	13.91	1.82
NI02	>50	>50	n.d.**	>50	>50	n.d.
Lopinavir	28.24	>50	>1.77	15.55	>50	>3.22
Chloroquine	85.12	>150	>1.76	11.69	>150	>12.83
Remdesivir	0.93	>50	>53.9	8.53	>50	>5.86

*Selective Index = CC_{50}/IC_{50}; **n.d., not determined.

Table S1. Anti-SARS-CoV-2 activity in Calu-3 and Vero cells.

3. Spectroscopic, mass & HPLC purity data

C01: ^{1}H NMR (600 MHz, $CD_3OD/CDCl_3$ = 1/1) δ 7.90–7.87 (m, 2H), 7.83–7.81 (m, 2H), 7.73–7.70 (m, 2H), 7.61–7.56 (m, 3H), 7.53–7.49 (m, 2H), 6.89 (s, 1H), 3.36–3.33 (m, 4H), 3.21–3.16 (m, 4H), 1.69 (s, 6H); ^{13}C NMR (150 MHz, $CD_3OD/CDCl_3$ = 1/1) δ 166.6, 162.9 (q, $^{2}J_{C,F}$ = 35.3 Hz), 151.4, 145.1, 143.1, 135.5, 134.6, 133.1, 132.6, 131.4 (q, $^{2}J_{C,F}$ = 32.7 Hz), 129.3, 127.4 (q, $^{3}J_{C,F}$ = 3.8 Hz), 127.4, 126.8, 126.1, 124.4 (q, $^{1}J_{C,F}$ = 270.4 Hz), 124.2, 118.5, 117.3 (q, $^{1}J_{C,F}$ = 291.0 Hz), 112.0, 110.9, 78.1, 49.1, 44.4, 28.7; HRMS(ESI^{+}) m/z calculated for $C_{30}H_{29}F_3N_5O_2$ $[M+H]^{+}$: 548.2268, found: 548.2264; HPLC purity = 95.76%.

C02: ^{1}H NMR (600 MHz, $CD_3OD/CDCl_3$ = 4/1) δ 7.91 (d, *J* = 8.3 Hz, 2H), 7.72 (d, *J* = 8.3 Hz, 2H), 7.61 (s, 1H), 7.31 (s, 1H), 7.24–7.19 (m, 2H), 7.18–7.12 (m, 3H), 6.75 (s, 1H), 3.23–3.18 (m, 4H), 2.97–2.88 (m, 6H), 2.60 (t, *J* = 7.2 Hz, 2H), 1.64 (s, 6H); ^{13}C NMR (150 MHz, $CD_3OD/CDCl_3$ = 4/1) δ 172.9, 163.0 (q, $^{2}J_{C,F}$ = 34.6 Hz), 151.9, 146.1, 143.8, 142.0, 136.1, 133.6, 131.7 (q, $^{2}J_{C,F}$ = 32.7 Hz), 129.3, 129.3, 127.8 (q, $^{3}J_{C,F}$ = 3.8 Hz), 127.4, 127.1, 125.9, 125.0 (q, $^{1}J_{C,F}$ = 270.2 Hz), 124.6, 119.8, 118.0 (q, $^{1}J_{C,F}$ = 285.9 Hz), 111.8, 110.7, 78.4, 49.1, 44.5, 39.2, 32.4, 28.7; HRMS(ESI^{+}) m/z calculated for $C_{32}H_{33}F_3N_5O_2$ $[M+H]^{+}$: 576.2581, found: 576.2573; HPLC purity =96.54%.

C03: ^{1}H NMR (500 MHz, $CD_3OD/CDCl_3$ = 1/1) δ 7.88 (d, J = 7.9 Hz, 2H), 7.73–7.68 (m, 3H), 7.58 (s, 1H), 7.50 (s, 1H), 7.43 (d, J = 5.0 Hz, 1H), 7.30 (d, J = 3.6 Hz, 1H), 7.09 (dd, J = 5.2, 3.7 Hz, 1H), 6.81 (s, 1H), 6.54 (d, J = 14.5 Hz, 1H), 3.38 (t, J = 5.1 Hz, 4H), 3.14 (t, J = 5.2 Hz, 4H), 1.68 (s, 6H); LRMS(ESI^{+}) m/z calculated for $C_{30}H_{29}F_3N_5O_2S$ $[M+H]^{+}$: 580.20, found: 580.20; HPLC purity = 94.01%.

C04: ^{1}H NMR (500 MHz, $CD_3OD/CDCl_3$ = 1/1)) δ 7.86 (d, *J* = 8.3 Hz, 2H), 7.68 (d, *J* = 8.2 Hz, 2H), 7.57 (s, 1H), 7.21 (s, 1H), 6.77 (s, 1H), 3.36–3.35 (m, 4H), 3.11 (t, *J* = 5.1 Hz, 4H), 2.31–2.24 (m, 1H), 1.85–1.78 (m, 2H), 1.78–1.70 (m, 4H), 1.67 (s, 6H), 1.49–1.33 (m, 4H); LRMS(ESI^{+}) m/z calculated for $C_{30}H_{35}F_3N_5O_2$ $[M+H]^{+}$: 554.27, found: 554.30; HPLC purity = 92.30%.

NI02: ^{1}H NMR (500 MHz, $CDCl_3$) δ 7.82 (d, J = 8.3 Hz, 2H), 7.65 (d, J = 8.2 Hz, 2H), 7.62 (s, 1H), 7.54 (s, 1H), 7.32–7.28 (m, 2H), 7.24–7.20 (m, 3H), 6.60 (s, 1H), 3.80 (t, J = 5.1 Hz, 2H), 3.55 (t, J = 5.0 Hz, 2H), 3.04 (t, J = 5.2 Hz, 2H), 3.02–2.97 (m, 2H), 2.89 (t, J = 5.0 Hz, 2H), 2.66 (t, J = 7.8 Hz, 2H), 1.70 (s, 6H); LRMS(ESI^{+}) m/z calculated for $C_{32}H_{31}F_3N_5O_4$ $[M+H]^{+}$: 606.23, found: 606.20; HPLC purity = 93.30%.

C05: LRMS(ESI$^+$) m/z calculated for $C_{28}H_{31}F_3N_5O_2$ $[M+H]^+$: 526.24, found: 526.25; HPLC purity = 75.86%.

C08: LRMS(ESI$^+$) m/z calculated for $C_{30}H_{36}F_3N_6O_2$ $[M+H]^+$: 569.28, found: 569.30; HPLC purity = 86.04%.

F03: LRMS(ESI$^+$) m/z calculated for $C_{28}H_{34}N_5O_2S$ $[M+H]^+$: 504.24, found: 504.25; HPLC purity = 85.46%.

C01 – ^{1}H NMR

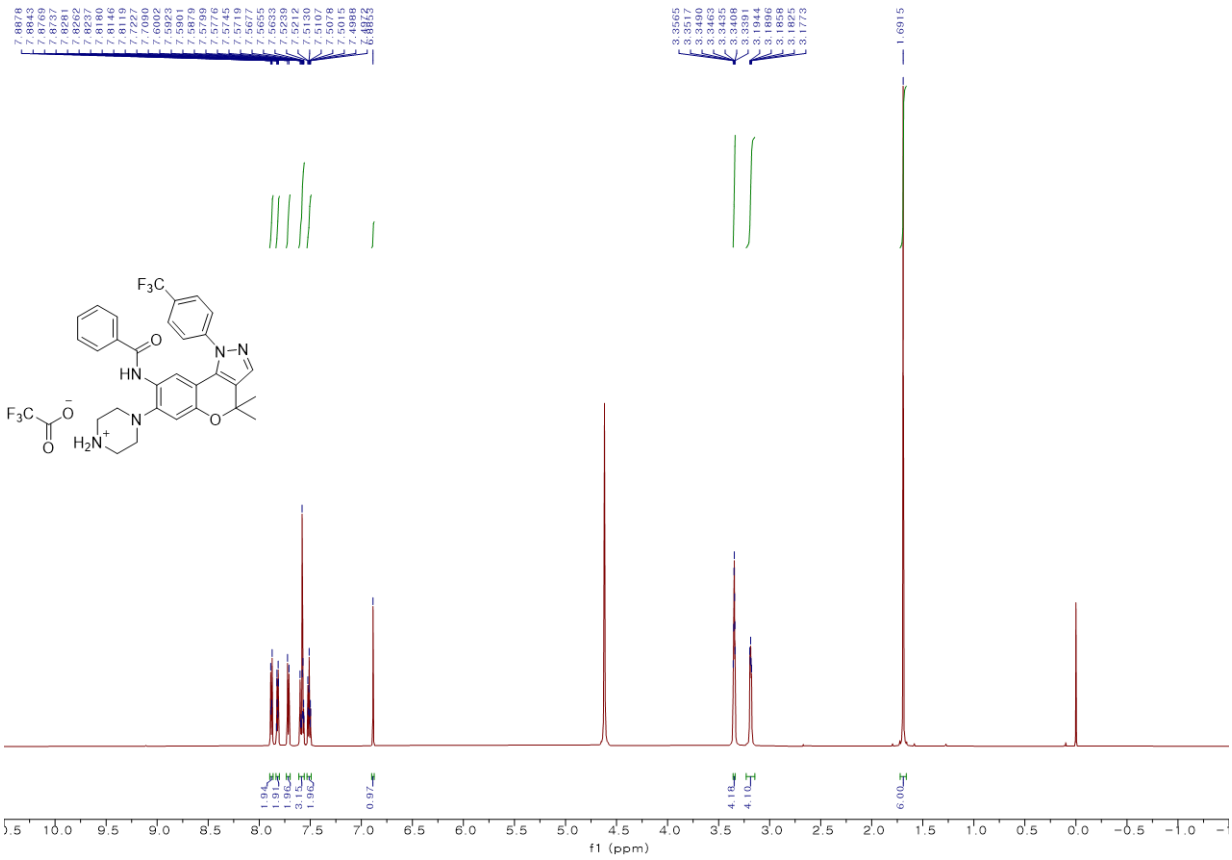

C01 – ^{13}C NMR

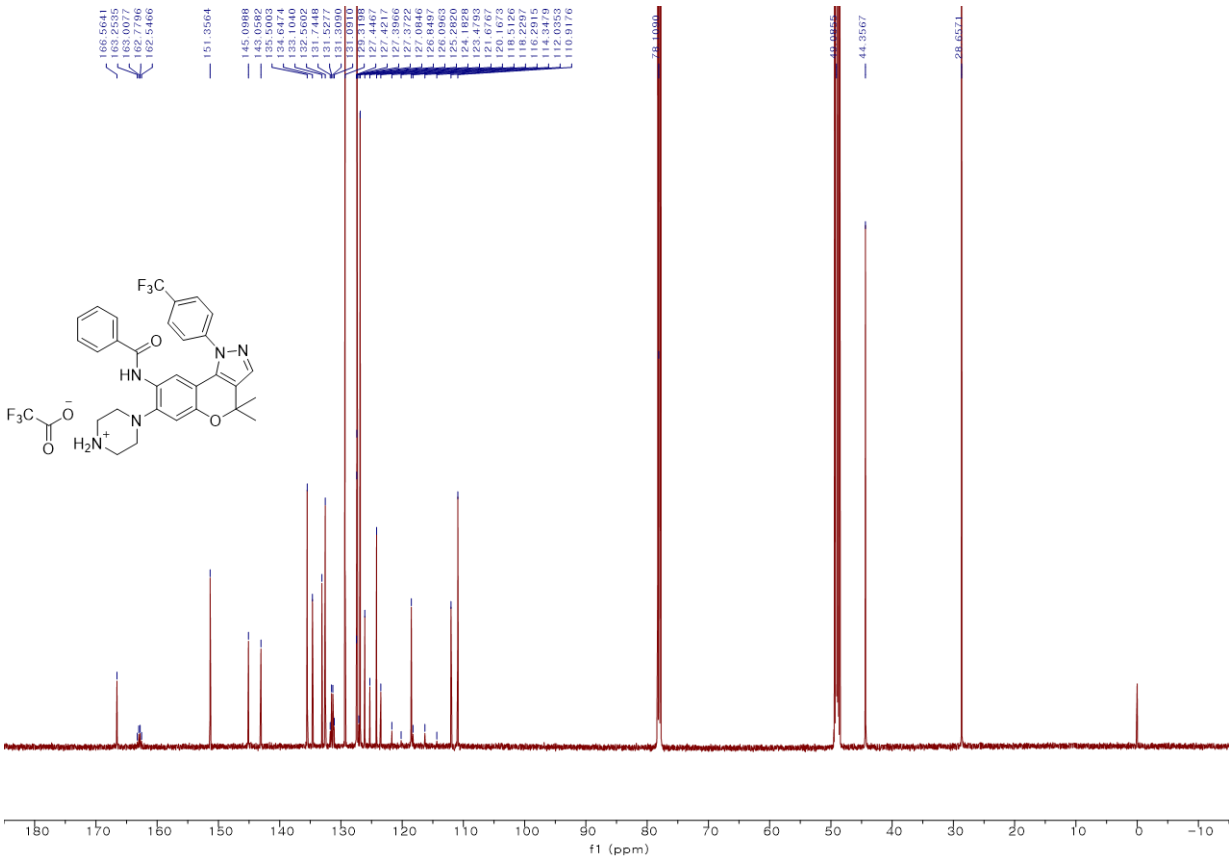

C02 – ^{1}H NMR

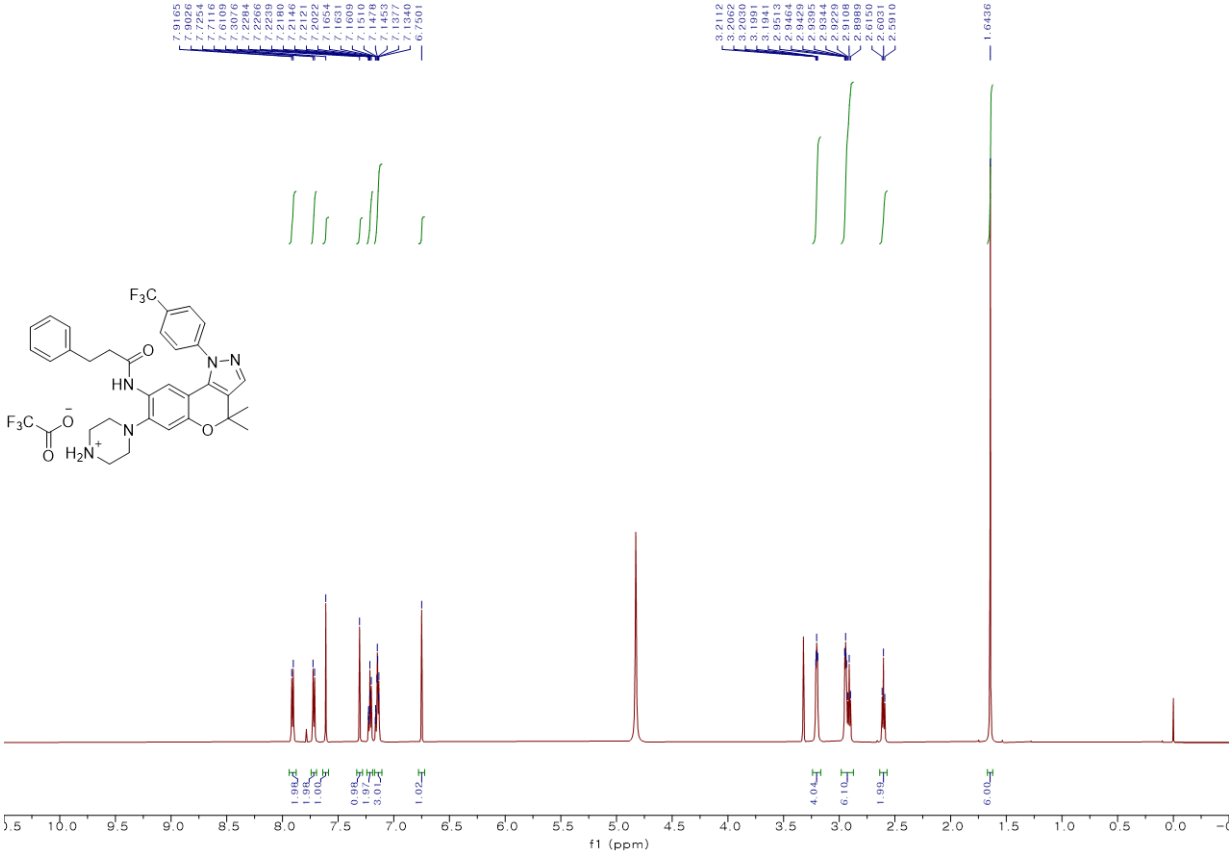

C02 – ^{13}C NMR

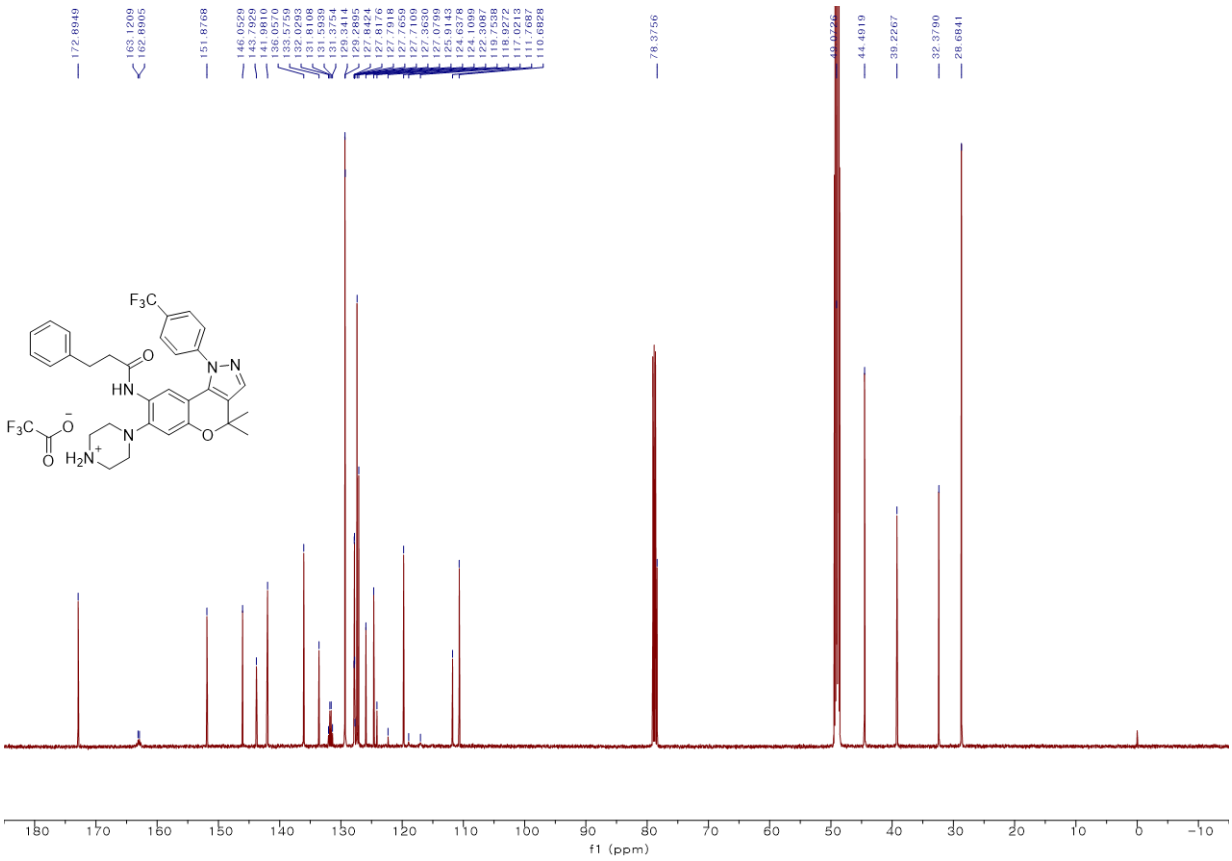

C03 – ^{1}H NMR

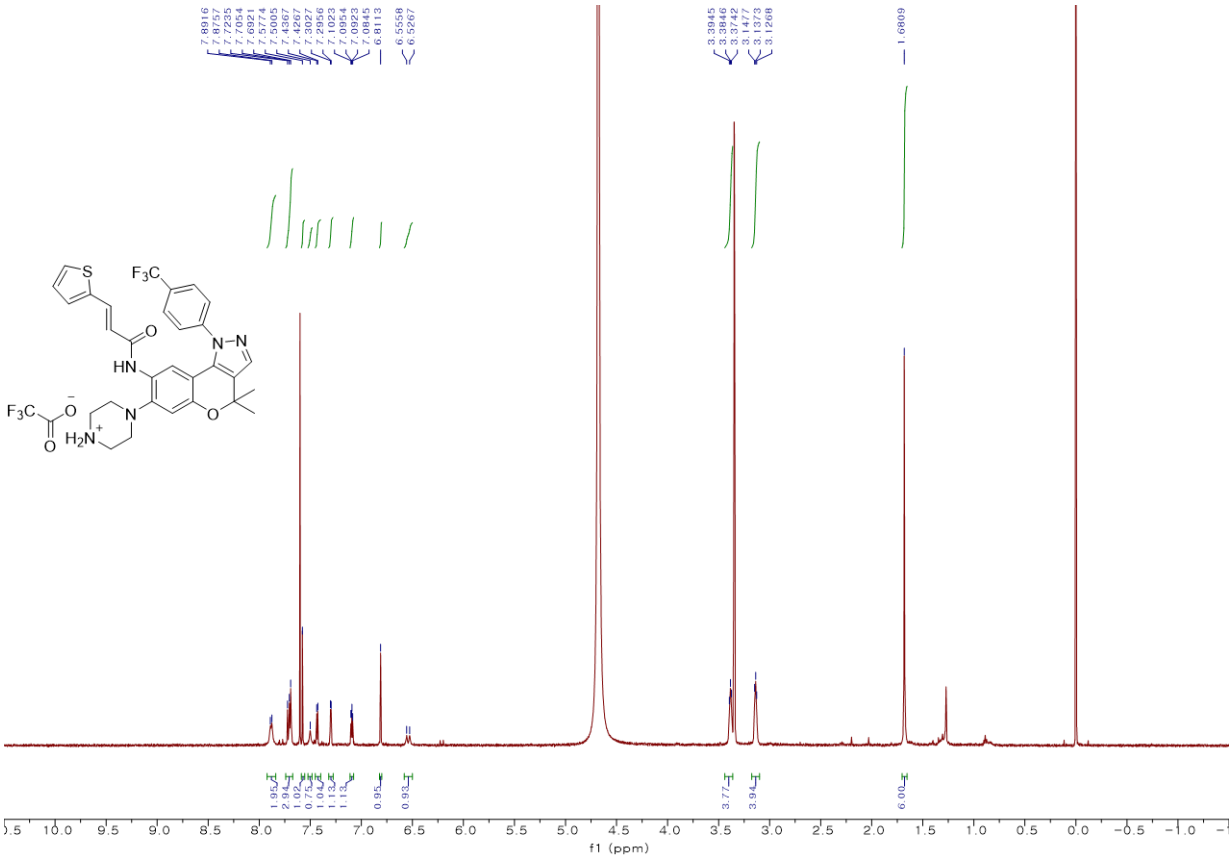

C04 – ^{1}H NMR

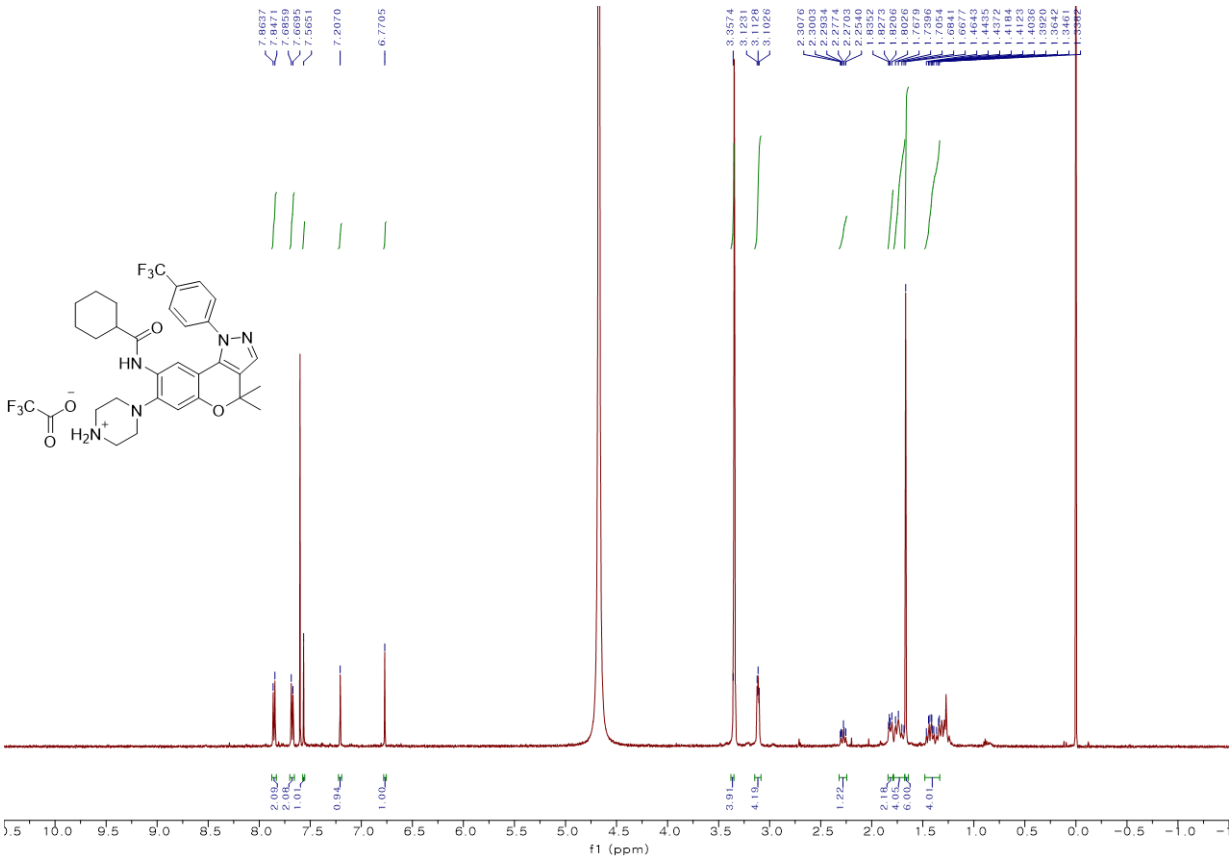

NI02 – ^{1}H NMR

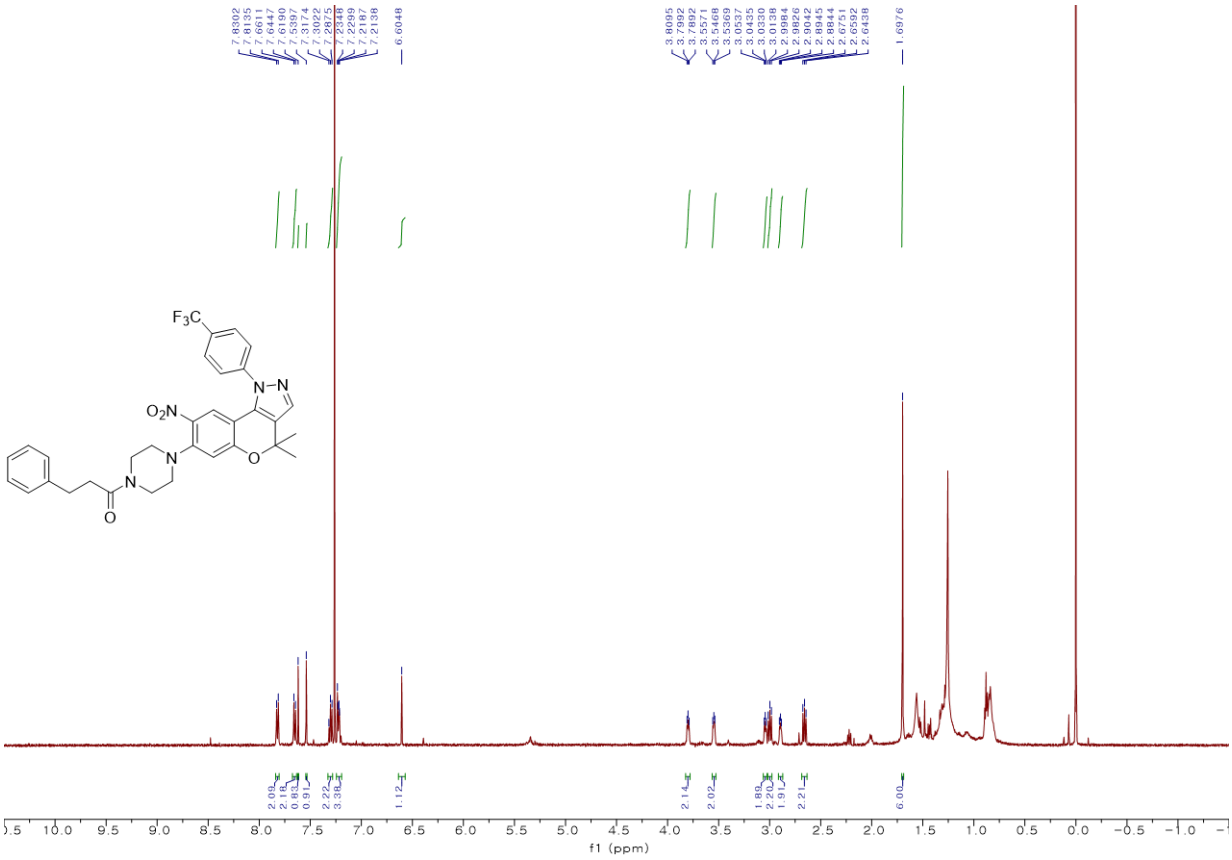

C01 – HPLC purity

95.76%

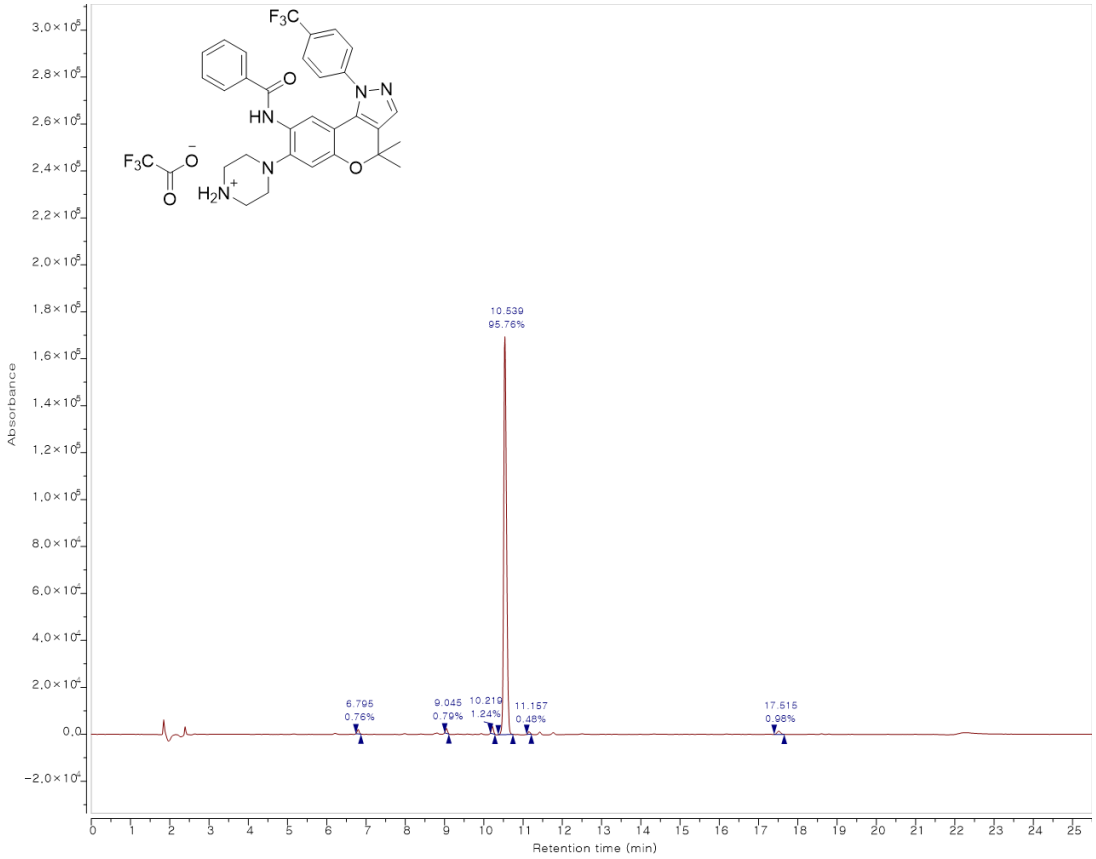

C02 – HPLC purity

96.54%

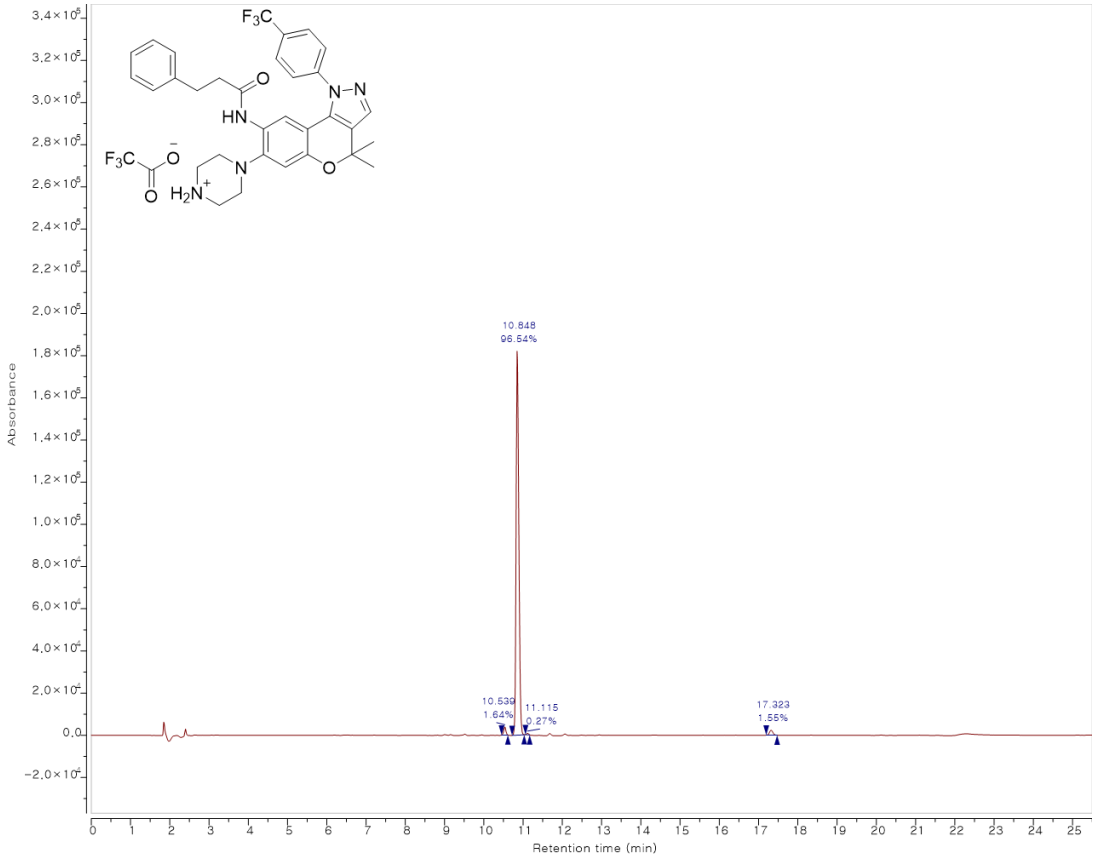

C03 – HPLC purity

94.01%

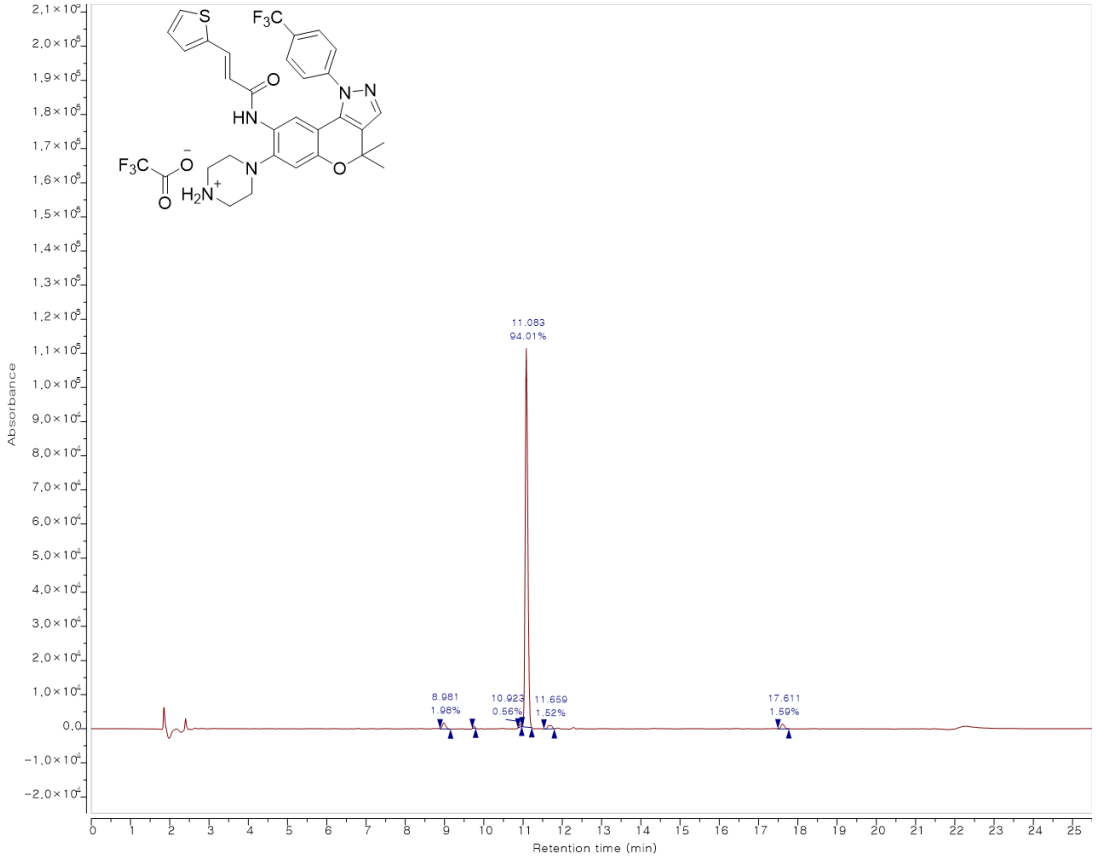

C04 – HPLC purity

92.30%

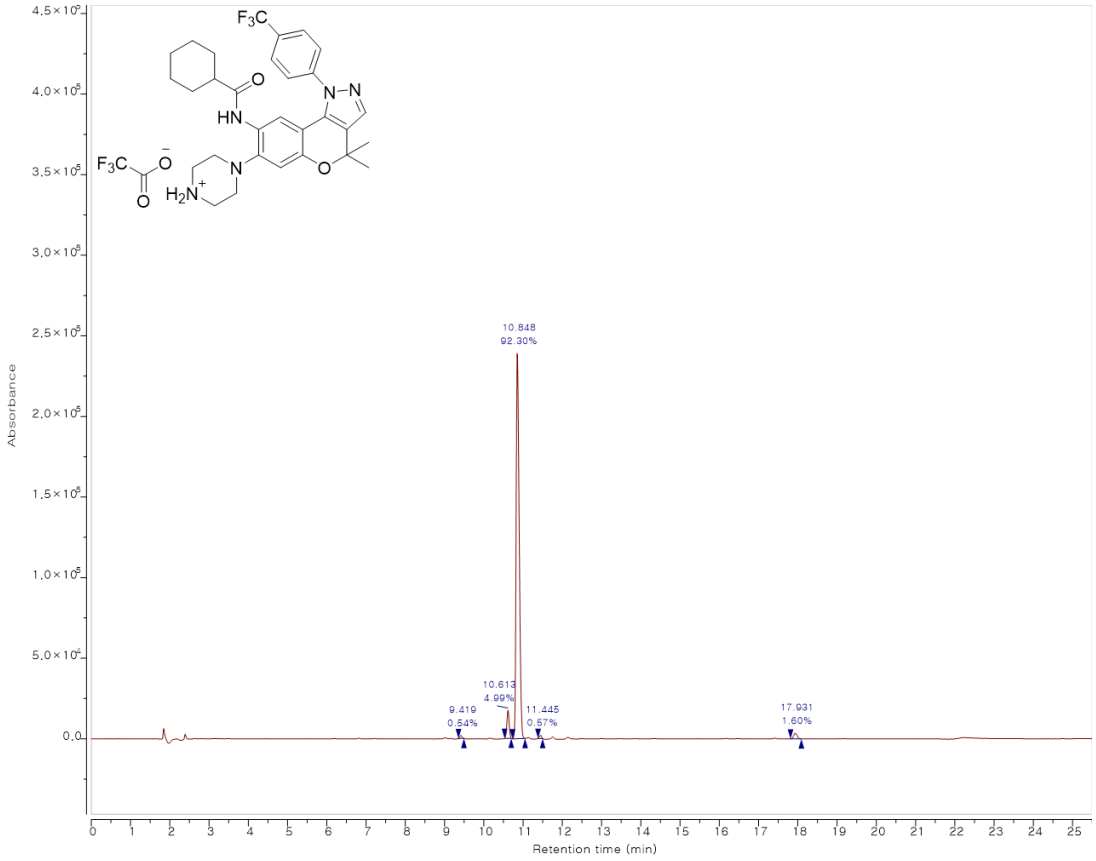

NI02 – HPLC purity

93.30%

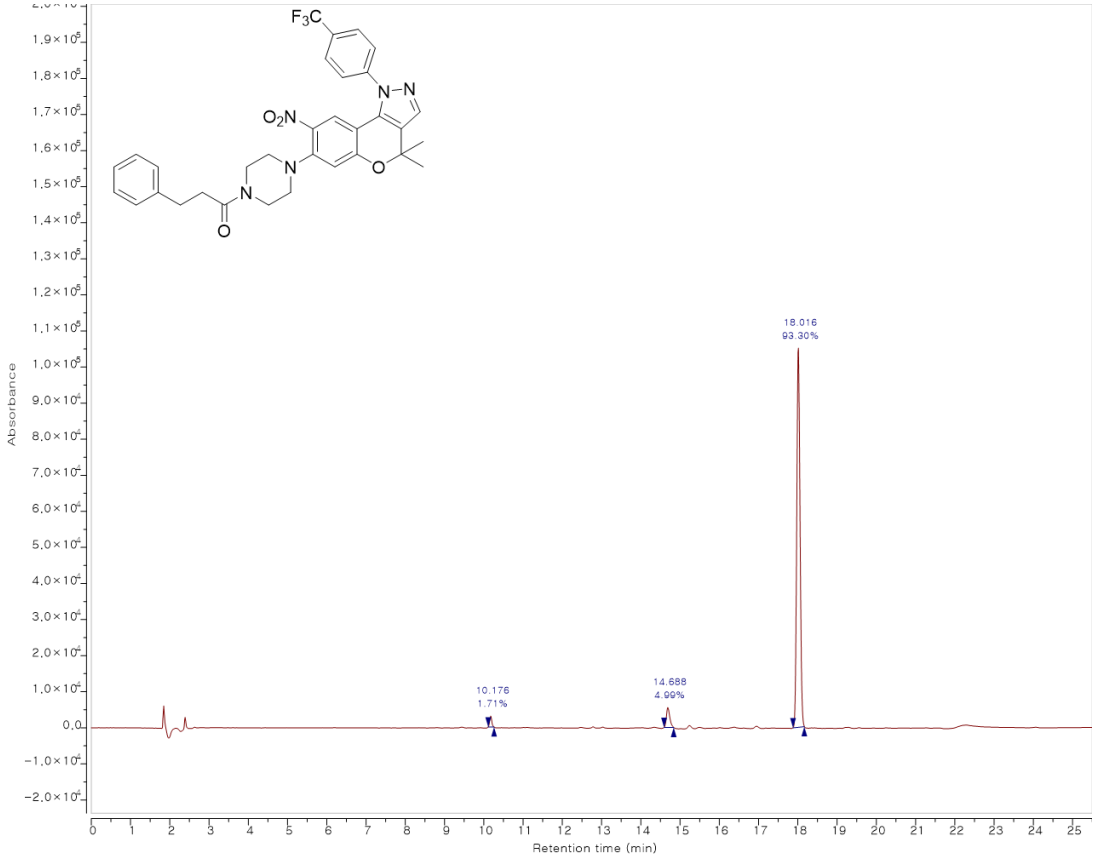

C05 – HPLC purity

75.86%

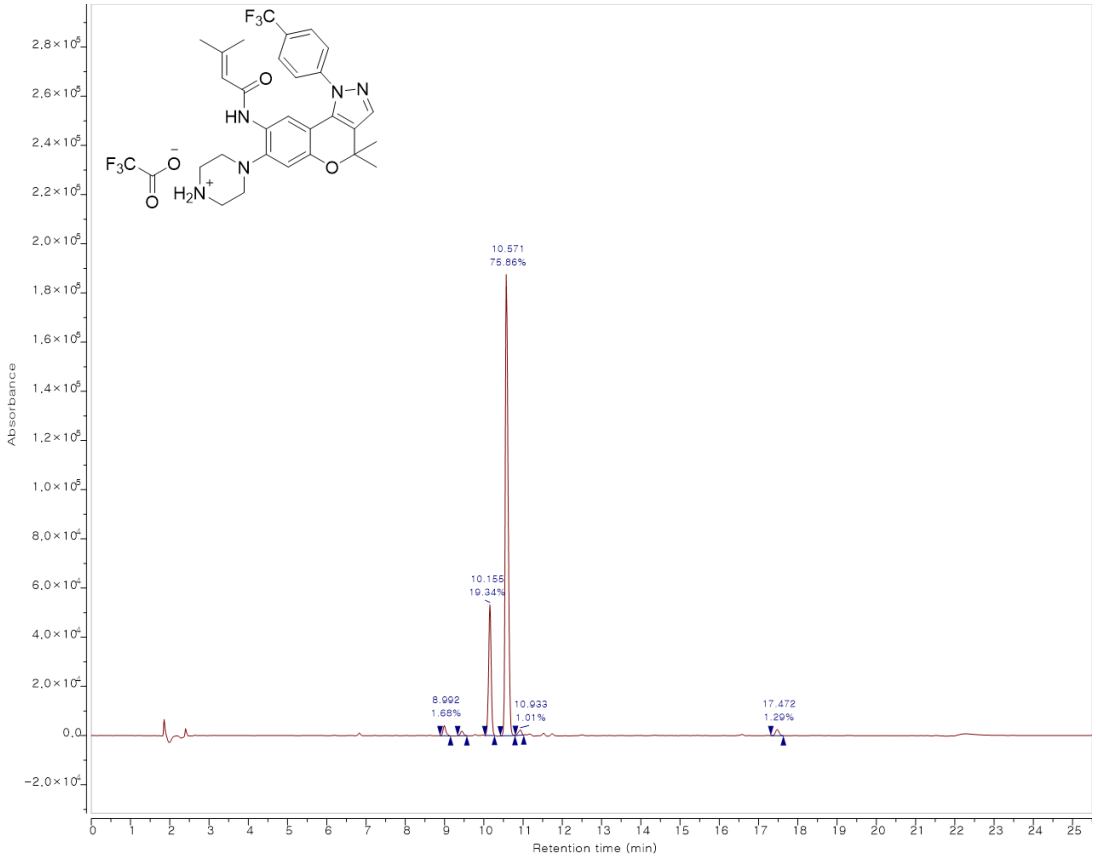

C08 – HPLC purity

86.04%

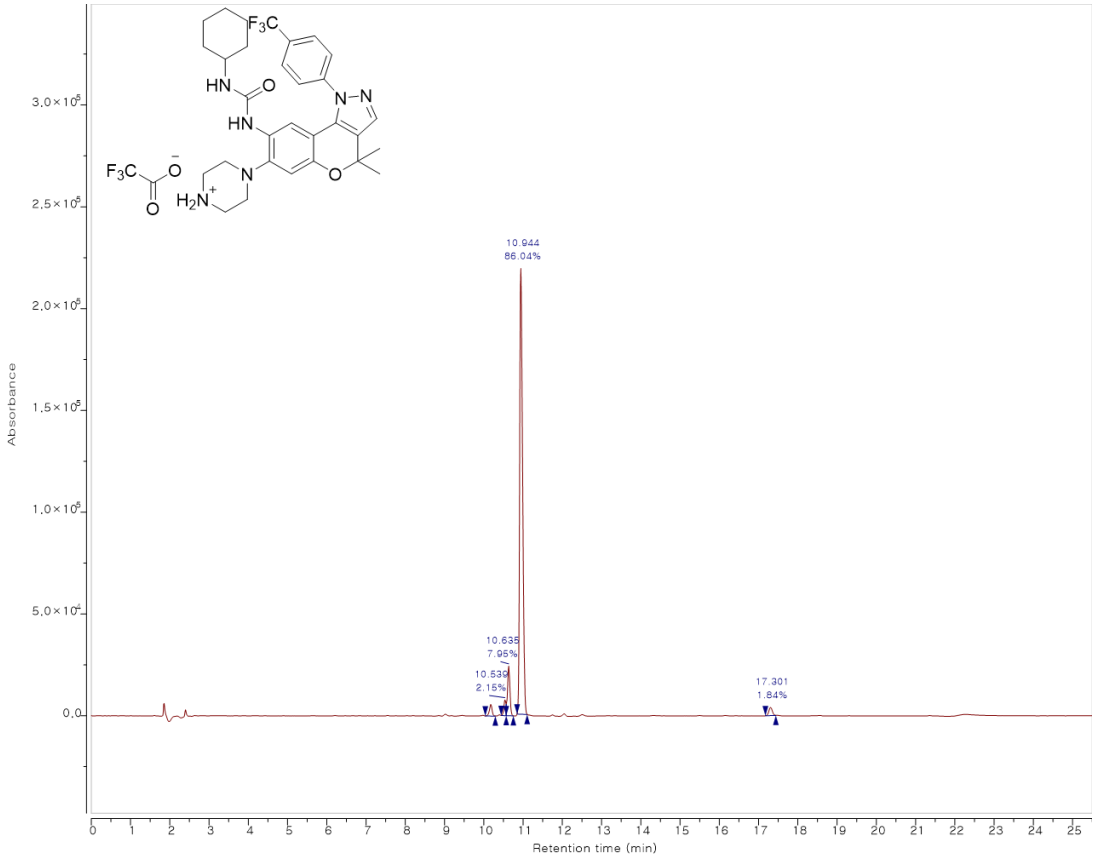

F03 – HPLC purity

85.46%

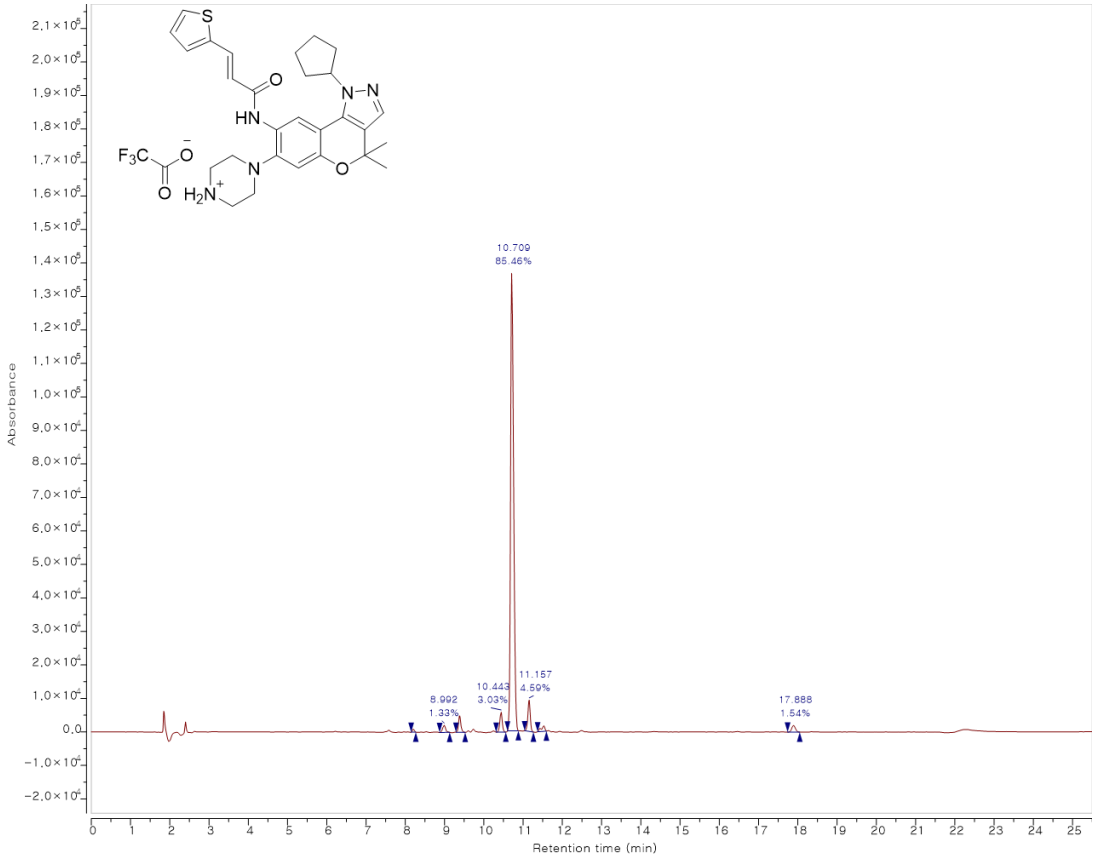

4. References

1. S. O. Park, J. Kim, M. Koh and S. B. Park, *J. Comb. Chem.* 2009, **11**, 315.